6 Solvent and Environmental Effects

Solvent polarity and the local environment have profound effects on the emission spectral properties of fluorophores. The effects of solvent polarity are one origin of the Stokes shift, which is one of the earliest observations in fluorescence. Emission spectra are easily measured, resulting in numerous publications on emission spectra of fluorophores in different solvents, and when bound to proteins, membranes, and nucleic acids. One common use of solvent effects is to determine the polarity of the probe binding site on the macromolecule. This is accomplished by comparison of the emission spectra and/or quantum yields when the fluorophore is bound to the macromolecule or dissolved in solvents of different polarity. However, there are many additional instances where solvent effects are used. Suppose a fluorescent ligand binds to a protein or membrane. Binding is usually accompanied by spectral shift or change in quantum yield due to the different environment for the bound ligand. Alternatively, the ligand may induce a spectral shift in the intrinsic or extrinsic protein fluorescence. In either case the spectral changes can be used to measure the extent of binding.

The effects of solvent and environment on fluorescence spectra are complex, and are due to several factors in addition to solvent polarity. The factors that affect fluorescence emission spectra and quantum yields include:

- Solvent polarity and viscosity
- Rate of solvent relaxation
- Probe conformational changes
- Rigidity of the local environment
- Internal charge transfer
- Proton transfer and excited state reactions
- Probe–probe interactions
- Changes in radiative and non-radiative decay rates

These multiple effects provide many opportunities to probe the local environment surrounding a fluorophore. However, it can be difficult to know which effect is dominant in a particular experimental system, and typically more than one effect will simultaneously affect the fluorophore.

When considering environmental effects, solvent polarity is usually the first topic. However, environmental effects as complex and even solvent polarity cannot be described using a single theory. The Lippert equation partially explains the effect of solvent polarity, but does not account for other effects such as hydrogen bonding to the fluorophore or internal charge transfer that depends on solvent polarity. In this chapter we will start with a description of general solvent effects, and then describe the other mechanisms that affect emission maxima and quantum yields.

6.1. OVERVIEW OF SOLVENT POLARITY EFFECTS

6.1.1. Effects of Solvent Polarity

Emission from fluorophores generally occurs at wavelengths that are longer than those at which absorption occurs. This loss of energy is due to a variety of dynamic processes that occur following light absorption (Figure 6.1). The fluorophore is typically excited to the first singlet state (S_1), usually to an excited vibrational level within S_1. The excess vibrational energy is rapidly lost to the solvent. If the fluorophore is excited to the second singlet state (S_2), it rapidly decays to the S_1 state in 10^{-12} s due to internal conversion. Solvent effects shift the emission to still lower energy due to stabilization of the excited state by the polar solvent molecules. Typically, the fluorophore has a larger dipole moment in the excited state (μ_E) than in the ground state (μ_G). Following excitation the solvent dipoles can reorient or relax around μ_E, which lowers the energy of the excited state. As the solvent polarity is increased, this effect becomes larger, resulting in emission at lower energies or longer wavelengths. In general, only fluorophores that are themselves polar display a large sensitivity to solvent polar-

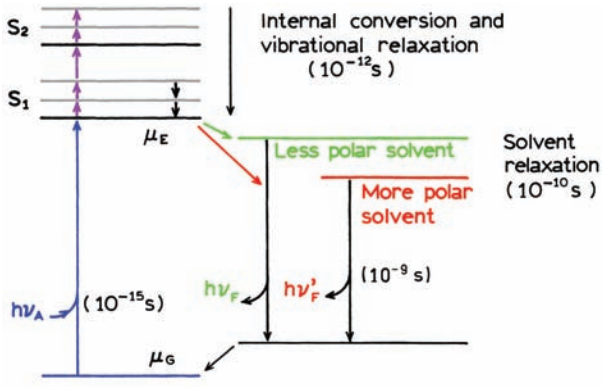

Figure 6.1. Jablonski diagram for fluorescence with solvent relaxation.

ity. Nonpolar molecules, such as unsubstituted aromatic hydrocarbons, are much less sensitive to solvent polarity.

Fluorescence lifetimes (1–10 ns) are usually much longer than the time required for solvent relaxation. For fluid solvents at room temperature, solvent relaxation occurs in 10–100 ps. For this reason, the emission spectra of fluorophores are representative of the solvent relaxed state. Examination of Figure 6.1 reveals why absorption spectra are less sensitive to solvent polarity than emission spectra. Absorption of light occurs in about 10^{-15} s, a time too short for motion of the fluorophore or solvent. Absorption spectra are less sensitive to solvent polarity because the molecule is exposed to the same local environment in the ground and excited states. In contrast, the emitting fluorophore is exposed to the relaxed environment, which contains solvent molecules oriented around the dipole moment of the excited state.

Solvent polarity can have a dramatic effect on emission spectra. Figure 6.2 shows a photograph of the emission from 4-dimethylamino-4'-nitrostilbene (DNS) in solvents of increasing polarity. The emission spectra are shown in the lower panel. The color shifts from deep blue (λ_{max} = 450 nm) in hexane to orange in ethyl acetate (λ_{max} = 600 nm), and red in n-butanol (λ_{max} = 700 nm).

6.1.2. Polarity Surrounding a Membrane-Bound Fluorophore

Prior to describing the theory of solvent effects it is helpful to see an example. Emission spectra of trans-4-dimethylamino-4'-(1-oxobutyl) stilbene (DOS) are shown in Figure 6.3.[1] The emission spectra are seen to shift dramatically to longer wavelengths as the solvent polarity is increased from cyclohexane to butanol. The sensitivity to solvent polarity is

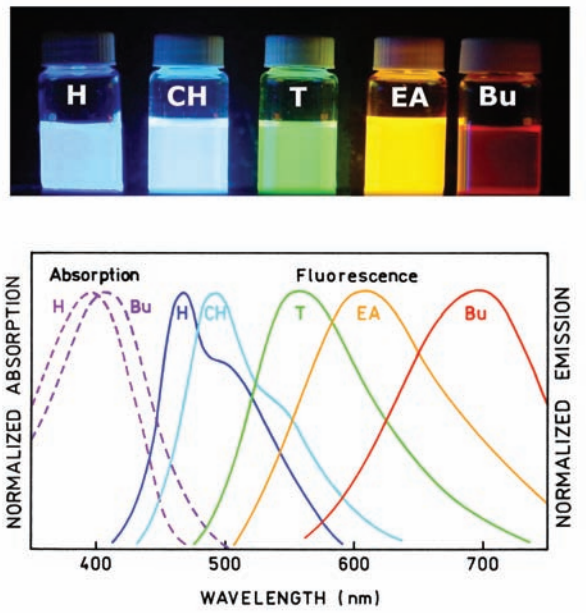

Figure 6.2. Photograph and emission spectra of DNS in solvents of increasing polarity. H, hexane; CH, cyclohexane; T, toluene; EA, ethyl acetate; Bu, n-butanol.

similar to DNS because of the similar electron-donating and -accepting groups on the fluorophore. The dimethyl amino group is the electron donor. The nitro group and carbonyl groups are both electron acceptors. The high sensitivity to solvent is due to a charge shift away from the amino groups in the excited state, towards the electron acceptor. This results in a large dipole moment in the excited state. This dipole moment interacts with the polar solvent molecules to reduce the energy of the excited state.

A typical use of spectral shifts is to estimate the polarity which surrounds the fluorophore. In Figure 6.3 the goal

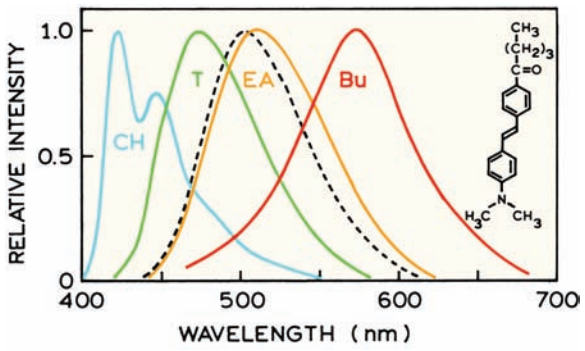

Figure 6.3. Corrected fluorescence emission spectra of DOS in cyclohexane (CH), toluene (T), ethyl acetate (EA), and butanol (Bu). The dashed line shows the emission of DOS from DPPC vesicles. Revised from [1].

was to determine the polarity of the DOS binding site on a model membrane that was composed of dipalmitoyl-L-α-phosphatidylcholine (DPPC). The emission spectrum of DOS bound to DPPC vesicles (dashed line) was found to be similar to that of DOS in ethyl acetate, which has a dielectric constant (ε) near 5.8. The polarity of the DOS binding site on DPPC vesicles is obviously greater than hexane (ε = 1.9) and less than butanol (ε = 17.8 at 20°C). Hence, the emission spectra of DOS indicate an environment of intermediate polarity for DOS when bound to DPPC vesicles.

6.1.3. Other Mechanisms for Spectral Shifts

While interpretation of solvent-dependent emission spectra appears simple, this is a very complex topic. The complexity is due to the variety of interactions that can result in spectral shifts. At the simplest level, solvent-dependent emission spectra are interpreted in terms of the Lippert equation (eq. 6.1, below), which describes the Stokes shift in terms of the changes in dipole moment which occur upon excitation, and the energy of a dipole in solvents of various dielectric constant (ε) or refractive index (n).[2–3] These general solvent effects occur whenever a fluorophore is dissolved in any solvent, and are independent of the chemical properties of the fluorophore and the solvent.

The theory for general solvent effects is often inadequate for explaining the detailed behavior of fluorophores in a variety of environments. This is because fluorophores often display multiple interactions with their local environment, which can shift the spectra by amounts comparable to general solvent effects. For instance, indole displays a structured emission in the nonpolar solvent cyclohexane (see Figure 16.5). This spectrum is a mirror image of its absorption spectrum. Addition of a small amount of ethanol (1 to 5%) results in a loss of the structured emission. This amount of ethanol is too small to significantly change solvent polarity and cause a spectral shift due to general solvent effects. The spectral shift seen in the presence of small amounts of ethanol is due to hydrogen bonding of ethanol to the imino nitrogen on the indole ring. Such specific solvent effects occur for many fluorophores, and should be considered while interpreting the emission spectra. Hence, the Jablonski diagram for solvent effects should also reflect the possibility of specific solvent–fluorophore interactions that can lower the energy of the excited state (Figure 6.4).

In addition to specific solvent–fluorophore interactions, many fluorophores can form an internal charge transfer (ICT) state, or a twisted internal charge transfer (TICT) state.[4] For instance, suppose the fluorophore contains both an electron-donating and an electron-accepting group. Such groups could be amino and carbonyl groups, respectively, but numerous other groups are known. Following excitation there can be an increase in charge separation within the fluorophore. If the solvent is polar, then a species with charge separation (the ICT state) may become the lowest energy state (Figure 6.4). In a nonpolar solvent the species without charge separation, the so-called locally excited (LE) state, may have the lowest energy. Hence, the role of solvent polarity is not only to lower the energy of the excited state due to general solvent effects, but also to govern which state has the lowest energy. In some cases formation of the ICT state requires rotation of groups on the fluorophore to form the TICT state. Formation of ICT states is not contained within the theory of general solvent effects. Additionally, a fluorophore may display a large spectral shift due to excimer or exciplex formation. The fluorophores may be

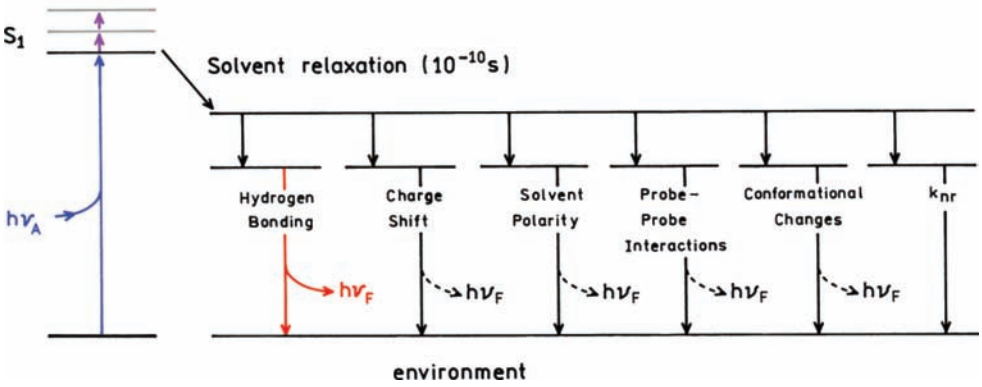

Figure 6.4. Effects of environment on the energy of the excited state. The dashed arrows indicate the fluorophore can be fluorescent or nonfluorescent in the different states.

fluorescent or nonfluorescent in these different states. The quantum yield can change due to change in the rate of non-radiative decay (k_{nr}) or due to a conformational change in the fluorophore.

In summary, no single theory can be used for a quantitative interpretation of the effects of environment on fluorescence. Interpretation of these effects relies not only on polarity considerations, but also on the structure of the fluorophore and the types of chemical interactions it can undergo with other nearby molecules. The trends observed with solvent polarity follow the theory for general solvent effects, which may give the impression that solvent polarity is the only factor to consider. In reality, multiple factors affect the emission of any given fluorophore.

6.2. GENERAL SOLVENT EFFECTS: THE LIPPERT-MATAGA EQUATION

The theory of general solvent effects provides a useful framework for consideration of solvent-dependent spectral shifts. In the description of general solvent effects the fluorophore is considered to be a dipole in a continuous medium of uniform dielectric constant (Figure 6.5). This model does not contain any chemical interactions, and hence cannot be used to explain the other interactions which affect the emission. These other interactions, such as hydrogen bonding or formation of charge transfer states, are sometimes detected as deviations from the general theory.

The interactions between the solvent and fluorophore affect the energy difference between the ground and excited states. To a first approximation this energy difference (in cm^{-1}) is a property of the refractive index (n) and dielectric constant (ε) of the solvent, and is described by the Lippert-Mataga equation:[2–3]

$$\bar{\nu}_A - \bar{\nu}_F = \frac{2}{hc}\left(\frac{\varepsilon - 1}{2\varepsilon + 1} - \frac{n^2 - 1}{2n^2 + 1}\right)\frac{(\mu_E - \mu_G)^2}{a^3} + \text{constant} \qquad (6.1)$$

In this equation h (= 6.6256 x 10^{-27} ergs) is Planck's constant, c (= 2.9979 x 10^{10} cm/s) is the speed of light, and a is the radius of the cavity in which the fluorophore resides. $\bar{\nu}_A$ and $\bar{\nu}_F$ are the wavenumbers (cm^{-1}) of the absorption and emission, respectively. Equation 6.1 is only an approximation, but there is reasonable correlation between the observed and calculated energy losses in non-protic solvents. By non-protic solvents we mean those not having hydroxyl groups, or other groups capable of hydrogen bonding. The Lippert equation is an approximation in which the polarizability of the fluorophore and higher-order terms are neglected. These terms would account for second-order effects, such as the dipole moments induced in the solvent molecules resulting by the excited fluorophore, and vice versa.

It is instructive to examine the opposite effects of ε and n on the Stokes shift. An increase in n will decrease this energy loss, whereas an increase in ε results in a larger difference between $\bar{\nu}_A$ and $\bar{\nu}_F$. The refractive index (n) is a high-frequency response and depends on the motion of electrons within the solvent molecules, which is essentially instantaneous and can occur during light absorption. In contrast, the dielectric constant (ε) is a static property, which depends on both electronic and molecular motions, the latter being solvent reorganization around the excited state. The different effects of ε and n on the Stokes shift will be explained in detail in Section 6.2.1. Briefly, an increase in refractive index allows both the ground and excited states to be instantaneously stabilized by movements of electrons within the solvent molecules. This electron redistribution results in a decrease in the energy difference between the ground and excited states (Figure 6.6). For this reason most chromophores display a red shift of the absorption spectrum in solvents relative to the vapor phase.[5–7] An increase in ε will also result in stabilization of the ground and excited states. However, the energy decrease of the excited state due to the dielectric constant occurs only after reorientation of the solvent dipoles. This process requires movement of

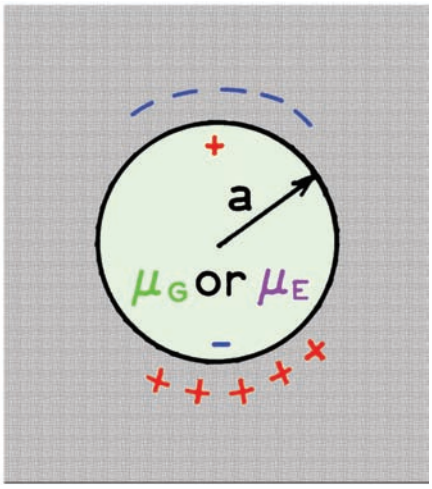

Figure 6.5. Dipole in a dielectric medium.

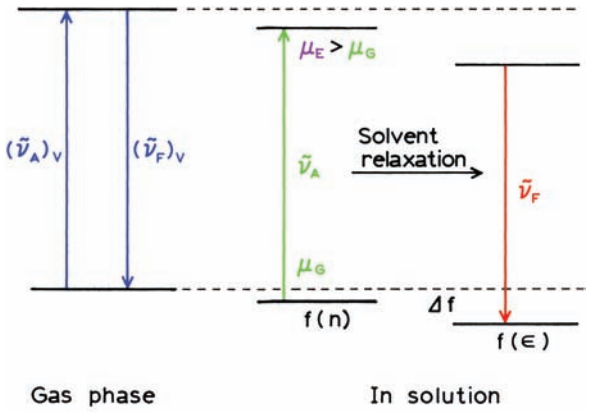

Figure 6.6. Effects of the refractive index (n) and dielectric constant (ε) on the absorption and emission energies.

the entire solvent molecule, not just its electrons. As a result, stabilization of the ground and excited states of the fluorophore depends on the dielectric constant (ε) and is time dependent. The rate of solvent relaxation depends on the temperature and viscosity of the solvent (Chapter 7). The excited state shifts to lower energy on a timescale comparable to the solvent reorientation time. In the derivation of the Lippert equation (Section 6.2.1), and throughout this chapter, it is assumed that solvent relaxation is complete prior to emission.

The term inside the large parentheses in eq. 6.1 is called the orientation polarizability (Δf). The first term $(\varepsilon - 1)/(2\varepsilon + 1)$ accounts for the spectral shifts due to both the reorientation of the solvent dipoles and to the redistribution of the electrons in the solvent molecules (Figure 6.6, center). The second term $(n^2 - 1)/(2n^2 + 1)$ accounts for only the redistribution of electrons. The difference of these two terms accounts for the spectral shifts due to reorientation of the solvent molecules (Figure 6.6, right), and hence the term orientation polarizability. According to this simple model, only solvent reorientation is expected to result in substantial Stokes shifts. The redistribution of electrons occurs instantaneously, and both the ground and excited states are approximately equally stabilized by this process. As a result, the refractive index and electronic redistribution has a comparatively minor effect on the Stokes shift.

It is instructive to calculate the magnitude of the spectral shifts that are expected for general solvent effects. Most fluorophores have nonzero dipole moments in the ground and excited states. As an example we will assume that the ground-state dipole moment is μ_G = 6D, and the excited-state dipole moment is μ_E = 20D, so that $\mu_E - \mu_G$ = 14D. We will also assume the cavity radius is 4 Å, which is comparable to the radius of a typical aromatic fluorophore. One Debye unit (1D) is 1.0 x 10^{-18} esu cm. 4.8D is the dipole moment that results from a charge separation of one unit charge (4.8 x 10^{-10} esu) by 1 Å (10^{-8} cm). An excited-state dipole moment of 20D is thus comparable to a unit charge separation of 4.2 Å, which is a distance comparable to the size of a fluorophore. These assumed values of μ_E and μ_G are similar to those observed for fluorophores which are frequently used as polarity probes in biochemical research.

For the model calculation of Stokes losses we compare the nonpolar solvent hexane with several polar solvents. Nonpolar solvents such as hexane do not have a dipole moment. Hence, there are no dipoles to reorient around the excited state of the fluorophore. This physical property of hexane is reflected by $\varepsilon \simeq n^2$ (Table 6.1). From eq. 6.1 one calculates a small value for the orientation polarizability (Δf), and $\bar{\nu}_A$ and $\bar{\nu}_F$ are expected to be small or zero. For example, if we assume that our model fluorophore absorbs at 350 nm, the emission in hexane is calculated to also be at 350 nm (Table 6.2). However, even in nonpolar solvents, absorption and emission maxima do not coincide this closely. Excitation generally occurs to higher vibrational levels, and this energy is rapidly dissipated in fluid solvents (10^{-12} s). Emission generally occurs to an excited vibrational level of the ground state. As a result, absorption and emission are generally shifted by an amount at least equal to the vibrational energy, or about 1500 cm^{-1}. These energy losses are accounted for by the constant term in eq. 6.1, and would shift emission of our model fluorophore to 370 nm.

In polar solvents such as methanol, substantially larger Stokes losses are expected. For example, our model fluorophore is expected to emit at 526 nm in this polar solvent (Table 6.2). This shift is due to the larger orientation polarizability of methanol, which is a result of its dipole moment. This sensitivity of the Stokes shift to solvent polarity is the reason why fluorescence emission spectra are frequently used to estimate the polarity of the environment surrounding the fluorophore.

Table 6.1. Polarizability Properties of Some Common Solvents

	Water	Ethanol	Ether	Hexane
ε	78.3	24.3	4.35	1.89
n	1.33	1.35	1.35	1.37
Δf	0.32	0.30	0.17	0.001

Table 6.2. Stokes Shifts Expected from General Solvent Effects

Solvent	ε	n	Δf[a]	$\bar{\nu}_A - \bar{\nu}_F$ (cm^{-1})[b]	λ_{max}[c] (nm)
Hexane	1.874	1.372	–0.0011[d]	35	350[d]
Chloroform	4.98	1.447	0.1523	4697	418.9
Ethyl Acetate	6.09	1.372	0.201	6200	447.0
1-Octanol	10.3	1.427	0.2263	6979	463.1
1-Butanol	17.85	1.399	0.2644	8154	489.8
n-Propanol	21.65	1.385	0.2763	8522	498.8
Methanol	33.1	1.326	0.3098	9554	525.8

[a]$\Delta f = [(\varepsilon - 1)/(2\varepsilon + 1)] - [(n^2 - 1)/(2n^2 + 1)]$.
[b]From eq. 6.1, assuming μ_G = 6D, μ_E = 20D, $\mu_E - \mu_G$ = 14D, and a cavity radius of 4 Å. 4.8D is the dipole moment that results from a charge separation of 1 unit of charge (4.8 x 10^{-10} esu) by 1 Å (10^{-8} cm). 1 x 10^{-18} esu cm is 1 Debye unit (1.0D).
[c]Assuming an absorption maximum of 350 nm.
[d]The small negative value of Δf was ignored.

6.2.1. Derivation of the Lippert Equation

The interactions responsible for general solvent effects are best understood by derivation of the Lippert equation. This equation can be written as

$$hc\Delta\bar{\nu} = hc(\bar{\nu}_A - \bar{\nu}_F) = \frac{2\Delta f}{a^3}(\mu_E - \mu_G)^2 + \text{const} \quad (6.2)$$

where $\Delta\bar{\nu}$ is the frequency shift (in cm^{-1}) between absorption and emission, Δf is the orientation polarizability, and μ_E and μ_G are the excited- and ground-state dipole moments, respectively. The Lippert equation is derived by consideration of the interaction of a fluorophore with the solvent, and the timescale of these interactions. We need to recall the Franck-Condon principle, which states that nuclei do not move during an electronic transition (10^{-15} s). In contrast, the electrons of the solvent molecules can redistribute around the new excited state dipole during this time span. In addition, because of the relatively long lifetime of the excited state (~10^{-8} s), the solvent molecules can orientate to their equilibrium position around the excited state of the fluorophore prior to emission.

Derivation of the Lippert equation starts with the consideration of a point dipole in a continuous dielectric medium (Figure 6.4). The energy of the dipole in an electric field given by

$$E_{dipole} = -\mu R \quad (6.3)$$

where R is the electric field.[8] In our case the electric field is the relative reactive field in the dielectric induced by the dipole. The reactive field is parallel and opposite to the direction of the dipole, and is proportional to the magnitude of the dipole moment,

$$R = \frac{2\mu}{a^3} f \quad (6.4)$$

In this equation f is the polarizability of the solvent and a is the cavity radius. The polarizability of the solvent is a result of both the mobility of electrons in the solvent and the dipole moment of the solvent molecules. Each of these components has a different time dependence. Reorientation of the electrons in the solvent is essentially instantaneous. The high frequency polarizability $f(n)$ is a function of the refractive index:

$$f(n) = \frac{n^2 - 1}{2n^2 + 1} \quad (6.5)$$

The polarizability of the solvent also depends on the dielectric constant, which includes the effect of molecular orientation of the solvent molecules. Because of the slower timescale of molecular reorientation, this component is called the low frequency polarizability of the solvent, and is given by

$$f(\varepsilon) = \frac{\varepsilon - 1}{2\varepsilon + 1} \quad (6.6)$$

The difference between these two terms is

$$\Delta f = \frac{\varepsilon - 1}{2\varepsilon + 1} - \frac{n^2 - 1}{2n^2 + 1} \quad (6.7)$$

and is called the orientation polarizability. If the solvent has no permanent dipole moment, $\varepsilon \simeq n^2$ and $\Delta f \sim 0$. Table 6.1 lists representative values of ε, n and Δf. From the magnitudes of Δf one may judge that spectral shifts $\Delta\bar{\nu}$ will be considerably larger in water than in hexane.

The interactions of a fluorophore with solvent can be described in terms of its ground- (μ_G) and excited-state (μ_E) dipole moments, and the reactive fields around these dipoles. These fields may be divided into those due to electronic motions (R_{el}^G and R_{el}^E) and those due to solvent reorientation (R_{or}^G and R_{or}^E). Assuming equilibrium around the dipole moments of the ground and excited states, these reactive fields are

$$R_{el}^G = \frac{2\,\mu_G}{a^3} f(n) \qquad R_{el}^E = \frac{2\mu_E}{a^3} f(n)$$

$$R_{or}^G = \frac{2\mu_G}{a^3}\Delta f \qquad R_{el}^E = \frac{2\mu_E}{a^3}\Delta f \tag{6.8}$$

Consider Figure 6.7, which describes these fields during the processes of excitation and emission. For light absorption the energies of the ground (E^G) and nonequilibrium excited (E^E) states are

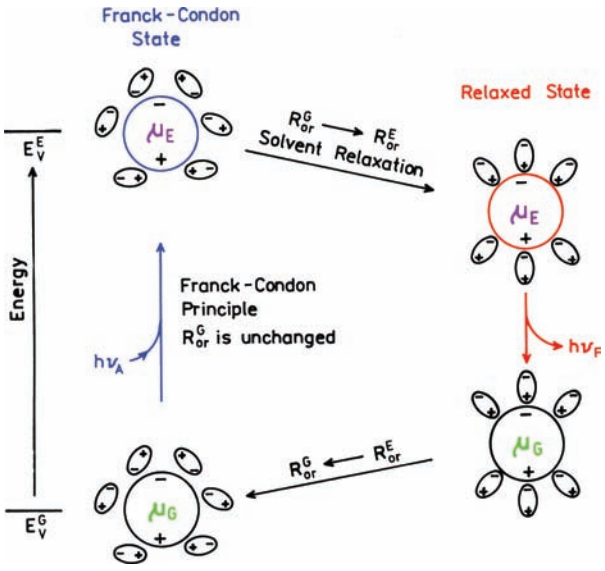

Figure 6.7. Effects of the electronic and orientation reaction fields on the energy of a dipole in a dielectric medium, $\mu_E > \mu_G$. The smaller circles represent the solvent molecules and their dipole moments.

$$\text{Energy}^E(\text{absorption}) = E_V^E - \mu_E R_{or}^G - \mu_E R_{el}^E \tag{6.9}$$

$$\text{Energy}^G(\text{absorption}) = E_V^G - \mu_G R_{or}^G - \mu_G R_{el}^G \tag{6.10}$$

where E_V represents the energy levels of the fluorophore in the vapor state, unperturbed by solvent. The absorption transition energy is decreased by the electronic reaction field induced by the excited state dipole. This occurs because the electrons in the solvent can follow the rapid change in electron distribution within the fluorophore. In contrast, the orientation of the solvent molecules does not change during the absorption of light. Therefore, the effect of the orientation polarizability, given by $\mu_G R_{or}^G$ and $\mu_E R_{or}^G$, contains only the ground-state orientational reaction field. This separation of effects is due to the Franck-Condon principle. Recalling that energy is related to the wavelength by $\bar{\nu} = \Delta E/hc$, subtraction of eq. 6.10 from 6.9 yields the energy of absorption:

$$hc\bar{\nu}_A = hc\,(\bar{\nu}_A)_V - (\mu_E - \mu_G)\,(R_{or}^G)$$

$$- \mu_E R_{el}^E + \mu_G R_{el}^G \tag{6.11}$$

where $hc(\bar{\nu}_A)_V$ is the energy difference in a vapor where solvent effects are not present. By a similar consideration one can obtain the energy of the two electronic levels for emission. These are

$$\text{Energy}^E(\text{emission}) = E_V^E - \mu_E R_{or}^E - \mu_E R_{el}^E \tag{6.12}$$

$$\text{Energy}^G(\text{emission}) = E_V^G - \mu_G R_{or}^E - \mu_G R_{el}^G \tag{6.13}$$

To derive these expressions we assumed that the solvent relaxed quickly in comparison to the lifetime of the excited state, so that the initial orientation field (R_{or}^G) changed to R_{or}^E prior to emission. The electronic field changed during emission, but the orientation field remained unchanged. The energy of the emission is given by

$$hc\bar{\nu}_F = hc(\bar{\nu}_F)_V - (\mu_E - \mu_G)R_{or}^E - \mu_E R_{el}^E + \mu_G R_{el}^G \tag{6.14}$$

In the absence of environmental effects one may expect $\bar{\nu}_A - \bar{\nu}_F$ to be a constant for complex molecules that undergo vibrational relaxation. Hence, subtracting eq. 6.14 from 6.11 yields

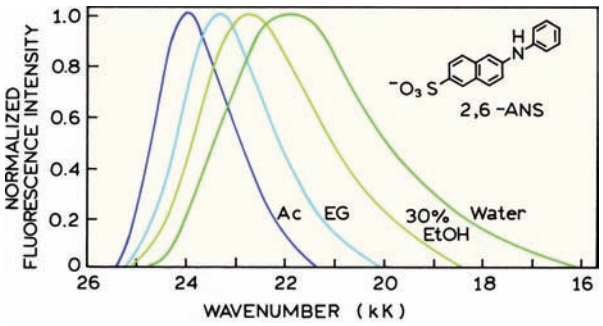

Figure 6.8. Normalized emission spectra for 6-anilino-2-naphthalene sulfonic acid (ANS). The solvents are acetonitrile (Ac), ethylene glycol (EG), 30% ethanol/70% water (30% EtOH), and water. 1 kK = 1000 cm^{-1}. Revised from [19].

$$\bar{\nu}_A - \bar{\nu}_F = -\frac{1}{hc}(\mu_E - \mu_G)(R_{or}^G - R_{or}^E) + \text{const} \quad (6.15)$$

Substitution from eq. 6.8 yields the Lippert equation:

$$\bar{\nu}_A - \bar{\nu}_F = \frac{-2}{hca^3}(\mu_E - \mu_G)(\mu_G \Delta f - \mu_E \Delta f) + \text{const} \quad (6.16)$$

$$\bar{\nu}_A - \bar{\nu}_F = \frac{2\Delta f}{hca^3}(\mu_E - \mu_G)^2 + \text{const} \quad (6.17)$$

It is important to remember that the Lippert equation is only an approximation, and contains many assumptions. The fluorophore is assumed to be spherical, and there is no consideration of specific interactions with the solvent. Other more complex equations have been presented, and the interested reader is referred to extensive publications on this subject.[9–14] In all these treatments the solvent is regarded as a continuum. The Lippert equation ignores the polarizability of the fluorophore and assumes that the ground and excited states dipole moments point in the same direction. If one assumes the polarizability of the fluorophore is the same as the solvent, and that μ_G and μ_E point in different directions, then if these directions are different, the Lippert equation become[13–14]

$$hc\Delta\bar{\nu} = \Delta b\left[\frac{\varepsilon - 1}{\varepsilon + 2} - \frac{n^2 - 1}{n^2 + 2}\right]\frac{(2n^2 + 1)}{(n^2 + 2)} + \text{const} \quad (6.18)$$

where

$$\Delta b = \frac{2}{hca^3}(\mu_G^2 - \mu_E^2 - \mu_G\mu_E\cos\alpha) \quad (6.19)$$

and α is the angle between μ_G and μ_E. It seems reasonable that general solvent effects would depend on the angle between μ_E and μ_G. However, it seems that the directions of the dipole moments are similar for many fluorophores in the ground and excited state. Given the fact that the spectral shifts due to specific solvent effects and formation of ICT states are often substantial, it seems preferable to use the simplest form of the Lippert equation to interpret the spectral data. Deviations from the predicted behavior can be used to indicate the presence of additional interactions.

To avoid confusion we note that eq. 6.18 was incorrect in the second edition of this book, as was pointed out in [15]. This equation was also incorrect on the original reports.[13–14]

6.2.2. Application of the Lippert Equation

The emission spectra of many fluorophores used to label macromolecules are known to be sensitive to solvent polarity. One of the best-known examples is the probe ANS. This class of probes has become widespread since its introduction in 1954.[16] ANS and similar molecules are essentially nonfluorescent when in aqueous solution, but become highly fluorescent in nonpolar solvents or when bound to proteins and membranes. These probes are highly sensitive to solvent polarity and can potentially reveal the polarity of their immediate environments.[17–19] For example, the emission maximum of 2,6-ANS shifts from 416 nm in acetonitrile to about 460 nm in water (Figure 6.8), and the emission maximum could be used to estimate the polarity of the binding site of ANS on the macromolecules.[20] Another reason for the widespread use of these probes is their low fluorescence in water. For example, the quantum yield of 1-anilinonaphthalene-8-sulfonate (1,8-ANS) is about 0.002 in aqueous buffer, but near 0.4 when bound to serum albumin. This 200-fold enhancement of the quantum yield is useful because the fluorescence of a dye–protein or dye–membrane mixture results almost exclusively from the dye that is bound to the biopolymers, with almost no contribution from the unbound probe. As a result, the spectral properties of the bound fraction may be investigated without interference from free dye.

The solvent sensitivity of a fluorophore can be estimated by a Lippert plot. This is a plot of $(\bar{\nu}_A - \bar{\nu}_F)$ versus the orientation polarizability (Δf). The most sensitive fluorophores are those with the largest change in dipole moment upon excitation. Representative Lippert plots for two naphthylamine derivatives are shown in Figure 6.9. The

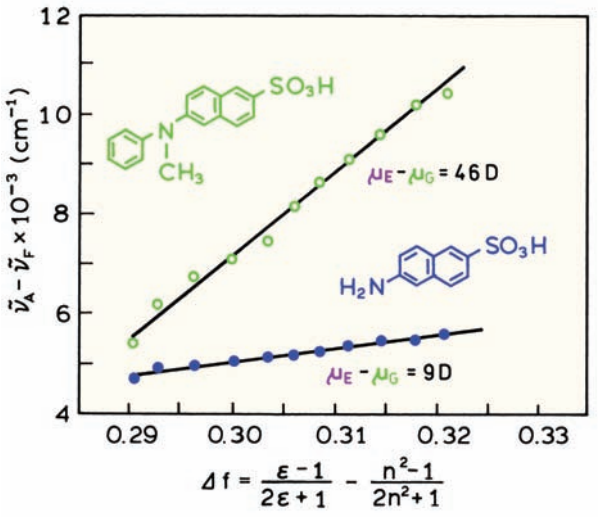

Figure 6.9. Lippert plots for two naphthylamine derivatives in ethanol–water mixtures. Data are shown for N-phenyl-N-methyl-6-aminonaphthalene-2-sulfonate (○) and 6-aminonaphthalene-2-sulfonate (●). Revised and reprinted with permission from [10]. Copyright © 1971, American Chemical Society.

sensitivity of these fluorophores to solvent polarity is probably due to a charge shift from the amino group towards the electronegative sulfonic acid group. The N-phenyl-N-methyl derivative of 6-aminonaphthalene-2-sulfonic acid is more sensitive to solvent polarity than the unsubstituted amino derivatives.[10] This higher sensitivity to solvent polarity is probably because the phenyl ring allows for a larger charge separation than the unsubstituted amino group.

The linearity of these plots is often regarded as evidence for the dominant importance of general solvent effects in the spectral shifts. Specific solvent effects lead to

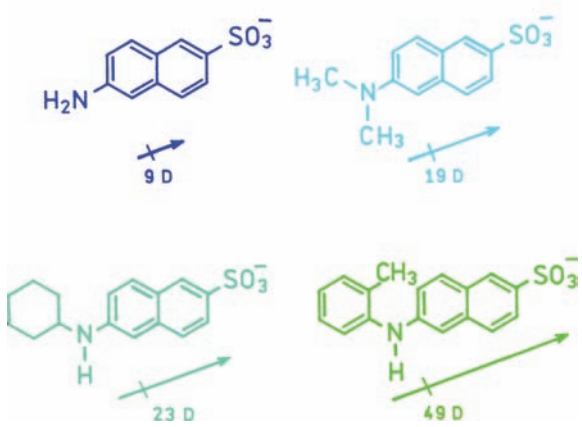

Figure 6.10. Chemical structure and change in dipole moment $\Delta\mu = \mu_E - \mu_G$ for naphthylamine derivatives.

nonlinear Lippert plots (Section 6.3). The data in Figure 6.9 are for a limited range of similar solvents. Specifically, these were ethanol–water mixtures, so the same specific effects due to hydrogen bonding were present in all mixtures. In general, the attachment of side chains to the amino group, especially aromatic groups, enhances the sensitivity to solvent polarity. This general trend can be seen from Figure 6.10, in which we show values of $(\mu_E - \mu_G)$ for several naphthylamine derivatives as determined from the Lippert plots. The change in dipole moment is large when electron-donating alkyl groups are attached to the nitrogen. Attachment of a toluyl group further increases the charge separation in the excited state.

6.3. SPECIFIC SOLVENT EFFECTS

In the preceding sections we described the general interactions between fluorophores and solvents, as modeled by the Lippert equation. These general effects are determined by the electronic polarizability of the solvent (which is described by the refractive index n) and the molecular polarizability (which results from reorientation of solvent dipoles). The latter property is a function of the static dielectric constant, ε. In contrast, specific interactions are produced by one or a few neighboring molecules, and are determined by the specific chemical properties of both the fluorophore and solvent.[21–22] Specific effects can be due to hydrogen bonding, preferential solvation, acid–base chemistry, or charge-transfer interactions, to name a few.[23–30] The spectral shifts due to such specific interactions can be substantial, and if not recognized, limit the detailed interpretation of fluorescence emission spectra.

Specific solvent–fluorophore interactions can often be identified by examining emission spectra in a variety of solvents. Typical data for 2-anilinonaphthalene (2-AN) in cyclohexane are shown in Figure 6.11. Addition of low concentrations of ethanol, which are too small to alter the bulk properties of the solvent, result in substantial spectral shifts.[19] Less than 3% ethanol causes a shift in the emission maximum from 372 to 400 nm. Increasing the ethanol concentration from 3 to 100% caused an additional shift to only 430 nm. A small percentage of ethanol (3%) caused 50% of the total spectral shift. Upon addition of the trace quantities of ethanol one sees that the intensity of the initial spectrum is decreased, and a new red-shifted spectrum appears. The appearance of a new spectral component is a characteristic of specific solvent effects. It is important to recognize that solvent-sensitive fluorophores can yield misleading infor-

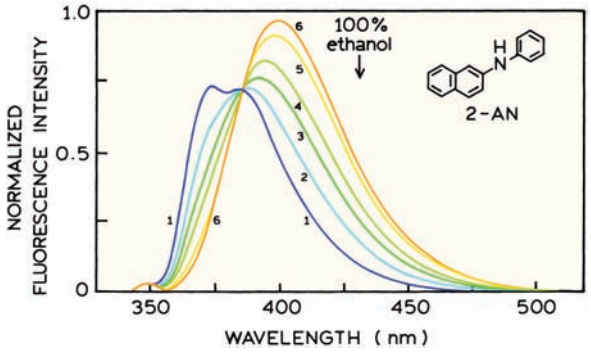

Figure 6.11. Fluorescence emission spectra of 2-anilinonaphthalene in cyclohexane, to which ethanol was added. These quantities were 0% (1), 0.2% (2), 0.4%, (3), 0.7% (4), 1.7% (5), and 2.7% (6). The arrow indicates the emission maximum in 100% ethanol. Revised and reprinted with permission from [19]. Copyright © 1971, Academic Press Inc.

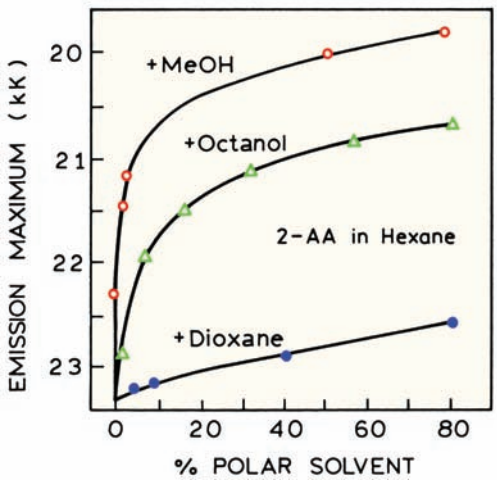

Figure 6.13. Effect of solvent composition on the emission maximum of 2-acetylanthracene. 1 kK = 1000 cm^{-1}. Revised from [32].

mation on the polarity of their environments if specific interactions occur, or if solvent relaxation is not complete. Because the specific spectral shift occurs at low ethanol concentrations, this effect is probably due to hydrogen bonding of ethanol to the amino groups, rather than general solvent effects.

Another example of specific solvent effects is provided by 2-acetylanthracene (2-AA) and its derivatives.[31–33] Emission spectra of 2-AA in hexane containing small amounts of methanol are shown in Figure 6.12. These low concentrations of ethanol result in a loss of the structured emission, which is replaced by a longer-wavelength unstructured emission. As the solvent polarity is increased further, the emission spectra continue a more gradual shift to longer wavelengths. These spectra suggest that the emission of 2-AA is sensitive to both specific solvent effects, and general solvent effects in more polar solvents.

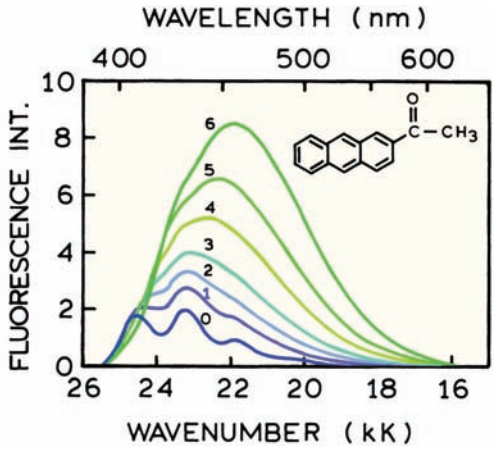

Figure 6.12. Fluorescence spectra of 2-acetylanthracene in methanol–hexane mixtures at 20°C. Concentrations of methanol in mol dm^{-3}: (0) 0, (1) 0.03, (2) 0.05, (3) 0.075, (4) 0.12, (5) 0.2, and (6) 0.34. Revised from [32].

The presence of specific solvent effects can be seen in the dependence of the emission maxima on the percentage of polar solvent (Figure 6.13). In hexane the emission maximum of 2-AA shifted gradually as the percentage of dioxane was increased to 100%. These shifts induced by dioxane are probably a result of general solvent effects. In contrast, most of the shift expected for methanol was produced by only about 1–2% methanol. This amount of alcohol is too small to affect the refractive index or dielectric constant of the solvent, and hence this shift is a result of specific solvent effects.

Specific solvent–fluorophore interactions can occur in either the ground state or the excited state. If the interaction only occurred in the excited state, then the polar additive would not affect the absorption spectra. If the interaction occurs in the ground state, then some change in the absorption spectrum is expected. In the case of 2-AA the absorption spectra showed loss of vibrational structure and a red shift upon adding methanol (Figure 6.14). This suggests that 2-AA and alcohol are already hydrogen bonded in the ground state. An absence of changes in the absorption spectra would indicate that no ground-state interaction occurs. Alternatively, weak hydrogen bonding may occur in the ground state, and the strength of this interaction may increase following excitation. If specific effects are present for a fluorophore bound to a macromolecule, interpretation

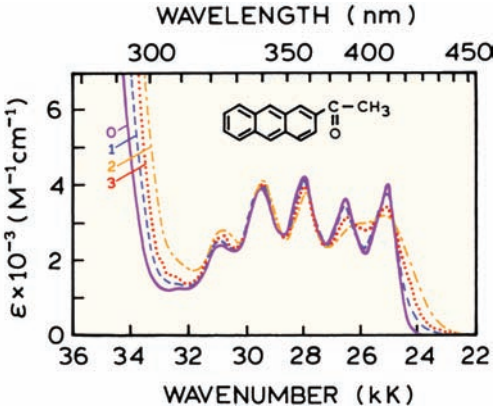

Figure 6.14. Absorption spectra of 2-acetylanthracene in pure hexane (0) and mixtures of methanol and hexane. The concentrations of methanol in mol dm^{-3} are 0.2 (1) and pure methanol (2). Spectrum 3 (dotted) refers to the H-bonded complex. Revised from [32].

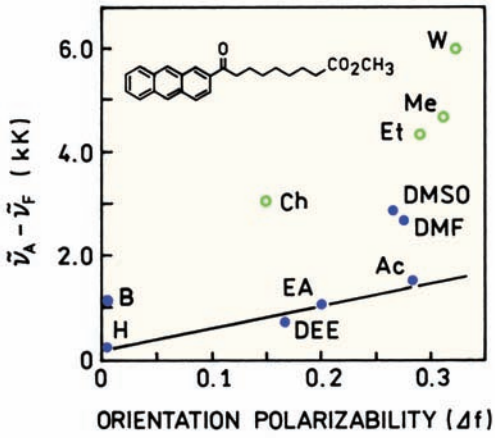

Figure 6.15. Stokes shifts of methyl 8-(2-anthroyl) octanoate in organic solvents and water. The solvents are benzene (B), n-hexane (H), diethyl ether (DEE), ethyl acetate (EA), acetone (Ac), N,N-dimethylformamide (DMF), chlorophorm (Ch), dimethyl sulfoxide (DMSO), ethanol (EA), methanol (Me), and water (W). Revised from [35]. Copyright © 1991, with permission from Elsevier Science.

of the emission spectrum is complex. For example, a molecule like 2-acetylanthracene, when bound in a hydrophobic site on a protein, may display an emission spectrum comparable to that seen in water if only a single water molecule is near the carbonyl group.

The presence of specific interactions in the ground state or only in the excited state determines the timescale of these interactions. If the fluorophore and polar solvent are already associated in the ground state, then one expects an immediate spectral shift upon excitation. If the fluorophore and polar solvent only associate in the excited state, then the appearance of the specific solvent effect will depend on the rates of diffusion of the fluorophore and polar solvent. In this case the dependence on the concentration of polar solvent will be similar to quenching reactions.

6.3.1. Specific Solvent Effects and Lippert Plots

Evidence for specific solvent–fluorophore interactions can be seen in the Lippert plots. One example is a long-chain fatty acid derivative of 2-AA. The compound was synthesized for use as a membrane probe.[34–35] One notices that the Stokes shift is generally larger in hydrogen bonding solvents (water, methanol, and ethanol) than in solvents that less readily form hydrogen bonds (Figure 6.15). Such behavior of larger Stokes shifts in protic solvents is typical of specific solvent–fluorophore interactions, and have been seen for other fluorophores.[36–38]

The sensitivity of fluorophores to specific interactions with solvents may be regarded as a problem, or a favorable circumstance. It is problematic because these effects can prevent a quantitative interpretation of the emission spectra in terms of the orientation polarizability of the macromolecule. The situation is favorable because the specific effects of protic solvents could reveal the accessibility of the macromolecule-bound probe to the aqueous phase. Also, specific solvent effects can cause larger and hence move easily observed spectral shifts.

In view of the magnitude of specific solvent effects, how can one reliably use fluorescence spectral data to indicate the polarity of binding sites? At present there seems to be no completely reliable method. However, by careful examination of the solvent sensitivity of a fluorophore, reasonable estimates can be made. Consider the following hypothetical experiment. Assume that 2-acetylanthracene (2-AA) binds strongly to lipid bilayers so that essentially all the 2-AA is bound to the membrane. It seems likely that, irrespective of the location of 2-AA in the bilayer, adequate water will be present, either in the ground state or during the excited-state lifetime, to result in saturation of the specific interactions shown in Figures 6.12 to 6.14. Under these conditions the solvent sensitivity of this fluorophore will be best represented by that region of Figure 6.13 where the concentration of the protic solvent is greater than 10–20%. Note that essentially equivalent slopes are found within this region for methanol, octanol and dioxane. These similar slopes indicate a similar mechanism, which is the general solvent effect.

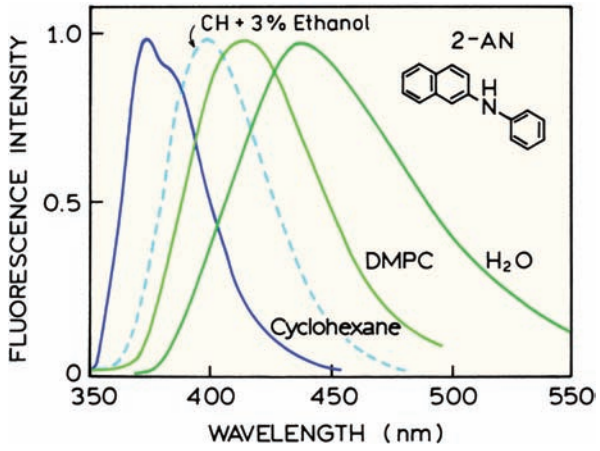

Figure 6.16. Normalized fluorescence emission spectra of 2-anilinonaphthalene in solvents and bound to vesicles of dimyristoyl-L-α-phosphatidylcholine (DMPC). The dashed line indicates the spectrum in cyclohexane (CH), which contains 3% ethanol. Revised from [39].

An understanding of specific and general solvent effects can provide a basis for interpreting the emission spectra of fluorophores that are bound to macromolecules. Consider the emission spectra of 2-anilinonaphthalene bound to membranes composed of dimyristoyl-L-α-phosphatidylcholine (DMPC).[39] The emission spectrum of 2-AN in DPMC is considerably red shifted relative to the emission in cyclohexane, but it is blue shifted relative to water (Figure 6.16). What is the polarity of the environment of 2-AN in the membranes? Interpretation of the emission maxima of these labeled membranes is also complicated by the time-dependent spectral shifts, a complication we will ignore for the moment. We noted earlier (Figure 6.11) that 2-AN is highly sensitive to small concentrations of ethanol. It seems likely that cyclohexane containing more than 3% ethanol is the preferable reference solvent for a low polarity environment. This spectrum is indicated by the dashed line in Figure 6.16. In this solvent the specific effects are saturated. With this adjustment in mind, one may conclude that the environment in which the 2-AN is localized is mostly nonpolar, but that this site is accessible to water. Without consideration of specific solvent effects one might conclude that the 2-AN is in a more polar environment.

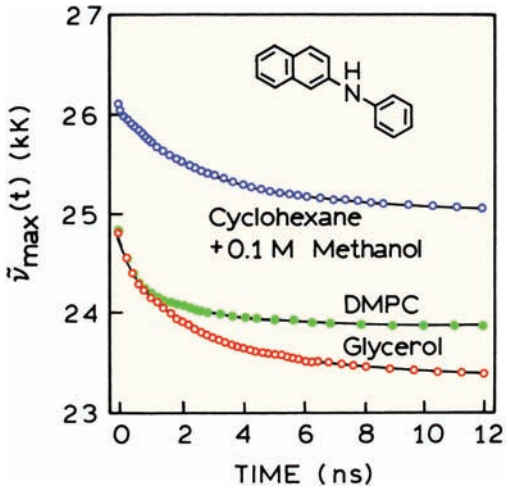

Figure 6.17. Time-resolved emission maxima of 2-anilinonaphthalene in DMPC vesicles and in solvents. Revised from [39].

The fact that the hydrogen bonding interactions of 2-AN are saturated in membranes is supported by time-resolved data. The measurement and interpretation of such data will be described in Chapter 7. Figure 6.17 shows the time-dependent emission maxima of 2-AN bound to DMPC vesicles, and in glycerol and cyclohexane. Even at the shortest observable time of one nanosecond, the emission maximum of 2-AN-labeled membranes is similar to that found in the protic solvent glycerol. This initial value for the emission maximum is also comparable to the completely relaxed value found for 2-AN in cyclohexane which contains 0.1 M methanol. This final value can be regarded as that expected when the specific solvent effects are saturated. This result indicates that in membranes the specific interactions with water or other polar hydrogen bonding groups are saturated. These interactions may have occurred in the ground state, or on a subnanosecond timescale that is too rapid to be resolved in this particular experiment. In either event, it seems clear that the emission spectra of 2-AN bound to model membranes can be interpreted more reasonably when compared to reference solvents in which the specific solvent effects are saturated.

6.4. TEMPERATURE EFFECTS

In the preceding sections we assumed that solvent relaxation was complete prior to emission, which is true for fluid solvents. At low temperatures the solvent can become more viscous, and the time for solvent reorientation increases. This is illustrated schematically in Figure 6.18, which shows a simplified description of solvent relaxation. Upon excitation the fluorophore is assumed to be initially in the Franck-Condon state (F). Solvent relaxation proceeds with a rate k_S. If this rate is much slower than the decay rate ($\gamma = 1/\tau$), then one expects to observe the emission spectrum of the unrelaxed F state. If solvent relaxation is much faster than the emission rate ($k_S >> \gamma$), then emission from the

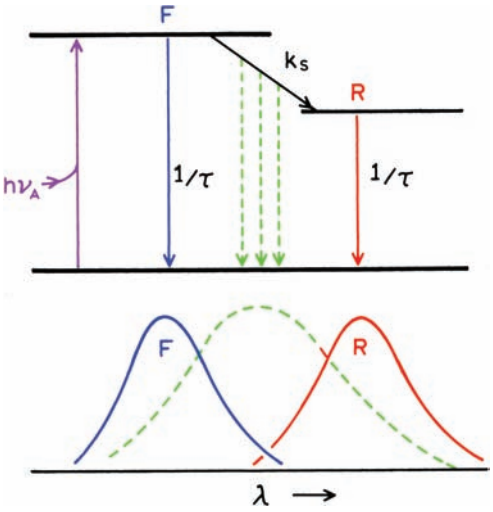

Figure 6.18. Jablonski diagram for solvent relaxation.

relaxed state (R) will be observed. At intermediate temperatures, where $k_S \simeq \gamma$, emission and relaxation will occur simultaneously. Under these conditions an intermediate emission spectrum will be observed. Frequently this intermediate spectrum (– – –) is broader on the wavelength scale because of contributions from both the F and R states. Time-dependent spectral relaxation is described in more detail in Chapter 7.

Examples of temperature-dependent emission spectra are shown in Figure 6.19 for the neutral tryptophan derivative N-acetyl-L-tryptophanamide (NATA) in propylene glycol. Solvents such as propylene glycol, ethylene glycol, and glycerol are frequently used to study fluorescence at low temperature. These solvents are chosen because their viscosity increases gradually with decreasing temperature, and they do not crystallize. Instead they form a clear highly viscous glass in which the fluorophores are immobilized. The presence of hydroxyl groups and alkyl chains makes these compounds good solvents for most fluorophores.

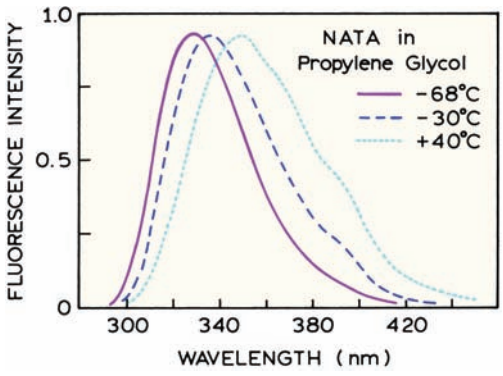

Figure 6.19. Emission spectra of N-acetyl-L-tryptophanamide (NATA) in propylene glycol. From [40].

As the temperature of NATA in propylene glycol is decreased the emission spectrum shifts to shorter wavelengths[40] (Figure 6.19). This shift occurs because the decay rate of fluorophores is not very dependent on temperature, but the relaxation rate is strongly dependent on temperature. Hence, at low temperature, emission is observed from the unrelaxed F state. It is important to notice that the structured ^1L_b (Chapter 16) emission of NATA is not seen even at the lowest temperature (–68°C). This is because the hydrogen bonding properties of propylene glycol persist at low temperature. It is clear that the temperature-dependent spectral shifts for NATA are due to the temperature dependence of the orientation polarizability Δf.

Another example of temperature-dependent spectra is provided by Patman (Figure 6.20).[42] This fluorophore is a lipid-like analogue of Prodan, which was developed to be a probe highly sensitive to solvent polarity.[42] The basic idea is that the amino and carbonyl groups serve as the electron donor and acceptor, respectively. In the excited state one expects a large dipole moment due to charge transfer (Figure 6.21), and thus a high sensitivity to solvent polarity. As the temperature of propylene glycol is decreased, the emission spectra of Patman shift dramatically to shorter wavelengths (Figure 6.20). The effects of low temperature are similar to those of low-polarity solvents. Because of the decreased rate of solvent motion, emission occurs from the unrelaxed state at low temperature.

6.5. PHASE TRANSITIONS IN MEMBRANES

Since its introduction as a solvent-sensitive probe, Prodan and its derivative have become widely used to label biomolecules.[43–46] Alkyl or fatty acid chains have been added to Prodan so that it localizes in membranes (Figure 6.22). Acrylodan is a derivative of Prodan that can be used to label sulfhydryl groups in proteins. Prodan is highly sensitive to solvent polarity. Its emission maximum shifts from 410 nm in cyclohexane to 520 nm in polar solvents (Figure 6.23).[47] Prodan and its derivatives have been especially useful for studies of cell membranes and model membranes because of its high sensitivity to the phase state of the membranes.[48–52] DPPC vesicles have a phase transition temperature near 37°. When Prodan is bound to DPPC vesicles the emission maximum shifts from 425 to 485 nm (Figure 6.24).

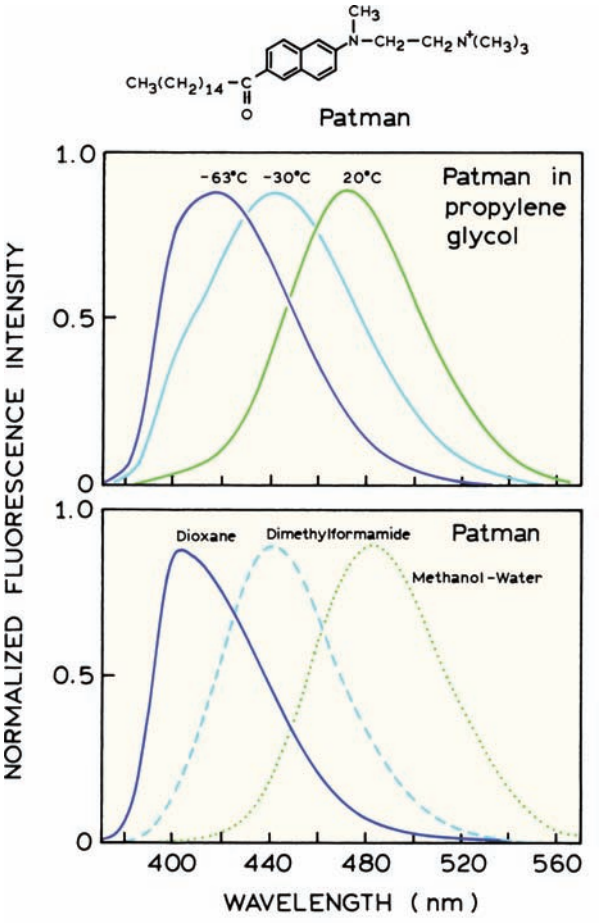

Figure 6.20. Emission spectra of the lipid-like Prodan derivative Patman at various temperatures in propylene glycol (top) and in solvents of different polarities (bottom). Revised and reprinted from [41]. Copyright © 1983, American Chemical Society.

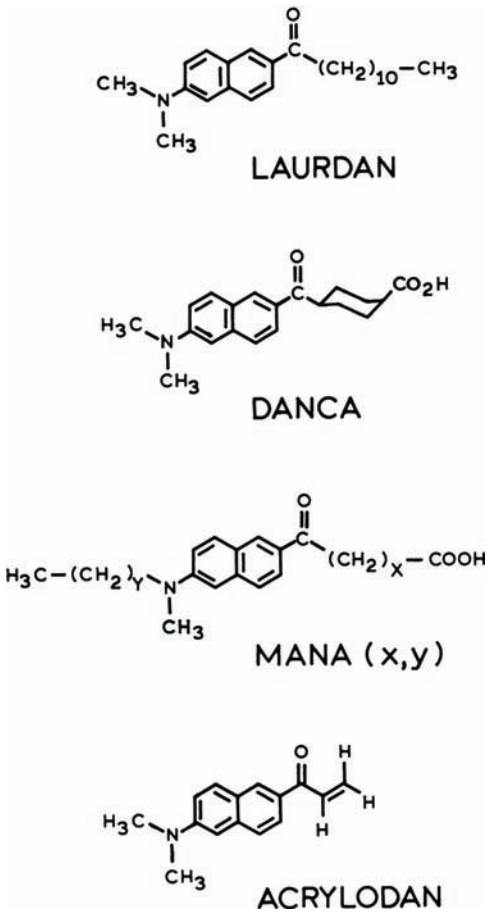

Figure 6.22. Derivatives of Prodan.

The large spectral shifts displayed by Prodan allowed its use in imaging the phase state of membranes.[53–54] When using fluorescence microscopy it is difficult to record the entire emission spectrum for each point in the image. The need for emission spectra was avoided by defining a wavelength-ratiometric parameter that represented the emission spectrum. This parameter is defined analogously to fluorescence polarization. This parameter was named the generalized polarization (GP) and is given by

$$GP = \frac{I_B - I_R}{I_B + I_R} \tag{6.20}$$

where I_B and I_R are the steady state intensities at a shorter blue (B) wavelength and a longer red (R) wavelength, respectively.

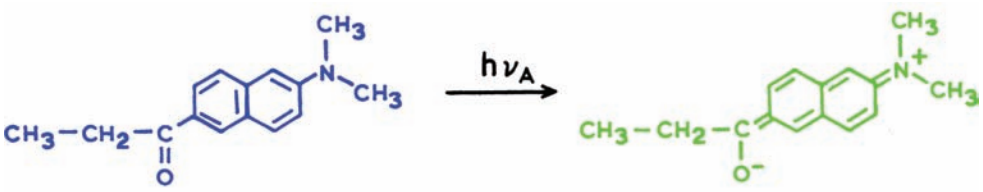

Figure 6.21. Charge separation in the excited state of Prodan (6-propionyl-2-(dimethylamino) naphthalene.

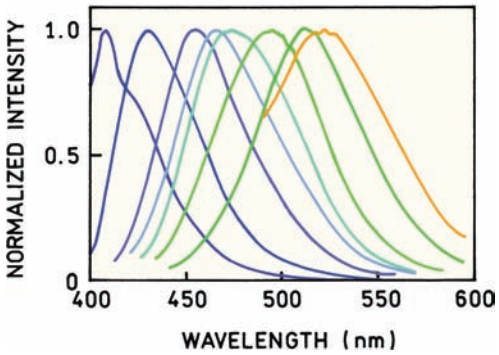

Figure 6.23. Emission spectra of Prodan in various solvents. From left to right the solvents are cyclohexane, toluene, CH_2Cl_2, CH_3CN, DMSO, isopropanol, methanol, and CF_3CH_2COOH. Revised and reprinted with permission from [47]. Copyright © 2003, American Chemical Society.

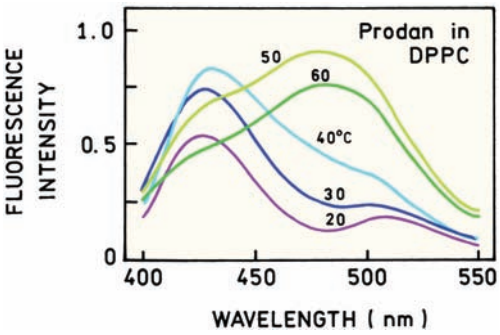

Figure 6.24. Emission spectra of Prodan in DPPC vesicles as a function of temperature. Revised from [50].

Giant unilamellar vesicles (GUVs) were formed from a mixture of DPPE and DPPC attached to Pt wires to hold them in position. The vesicles were labeled with the lipophilic probe Laurdan. Excitation was accomplished using a two-photon process, which eliminates out-of-focus fluorescence. Figure 6.25 shows the GP images of the vesicles at several temperatures. At 40°C the GP values are high (near 0.5) because the membrane is in the solid phase with more intense emission at short wavelengths. As the temperature is increased GP decreases and even becomes slightly negative due to the increased intensity at longer wavelengths.

In Figure 6.25 the phase state and GP values were rather constant throughout the GUV. However, real membranes are expected to be less homogeneous and to display rafts or domains that are either in the fluid or solid state. The sensitivity of Laurdan to the phase of the membrane allowed its use for imaging of domains in living cells. Figure 6.26 shows GP images of fibroblasts that were taken off the top of the cell (left) and from the region of the cell in contact with the glass slide (right). These images show regions of high GP, typically at protrusions of the membrane or points of contact with the glass slide. These results show how the spectroscopic studies of polarity effects can now be used for cellular imaging.

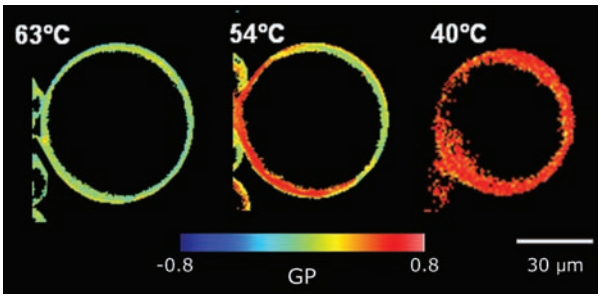

Figure 6.25. Generalized polarization of Laurdan in GUV of DPPE/DPPC 7:3 obtained with two-photon excitation at 780 nm. The blue and red intensities needed to calculate GP were measured through 46 nm wide bandpass filters centered at 446 and 499 nm, respectively. Reprinted from [53]. Courtesy of Dr. Luis Bagatolli.

6.6. ADDITIONAL FACTORS THAT AFFECT EMISSION SPECTRA

6.6.1. Locally Excited and Internal Charge-Transfer States

Depending upon solvent polarity some fluorophores can display emission before or after charge separation. One example is shown in Figure 6.27. The initially excited state is called the locally excited (LE) state. In low-polarity solvents FPP emits at short wavelengths from the LE state (top

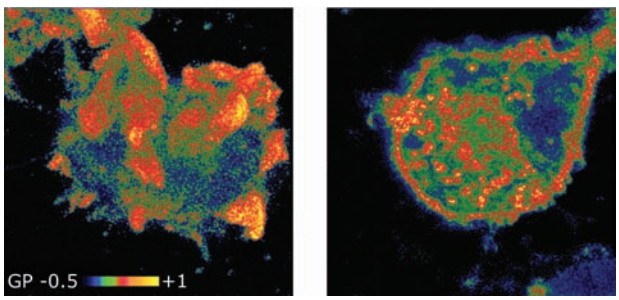

Figure 6.26. Generalized polarization of Laurdan in fibroblasts observed with two-photon excitation. The images were taken from above (left) and below (right) the glass slide. Reprinted from [54]. Courtesy of Dr. Katharina Gaus from the University of New South Wales, Australia.

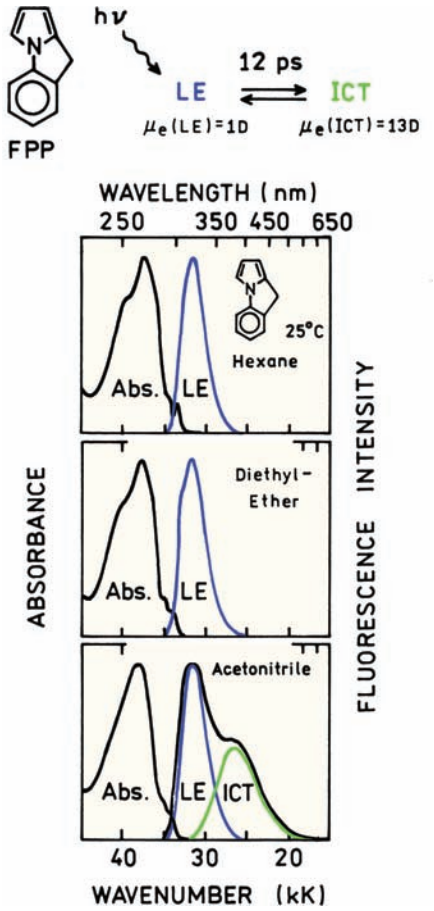

Figure 6.27. Emission spectra of FPP in several solvents. Revised and reprinted with permission from [55]. Copyright © 2004, American Chemical Society.

two panels). As the solvent polarity increases a new longer wavelength emission appears. This longer-wavelength emission (lower panel) is due to an internal charge-transfer (ICT) state, which forms rapidly following excitation. In this case the two ends of the fluorophore are held rigidly by the methylene bridge, so that formation of the ICT state does not depend on the twisting. There have been a large number of papers on conformational changes in the excited-state fluorophore to form a twisted internal charge transfer (TICT) state in a variety of molecules. There seems to be a lack of agreement on the need for twisting. To avoid stating an opinion on this topic, we will simply refer to such states as ICT states.

Another example of LE and ICT emission is given by Laurdan.[56] Part of the large spectral shift displayed by Laurdan is due to emission from the locally excited state (LE), which occurs near 400 nm, as well as from an ICT state emitting at longer wavelengths. A hint of this behavior was seen in Figure 6.20 (top), where at –30°C a shoulder appeared on the short-wavelength side of the Patman emission. Such changes in spectral shape often indicate the presence of another state. This new blue-emitting state was more easily seen in ethanol at low temperatures (Figure 6.28). As the temperature is decreased the emission maximum shifts from about 490 to 455 nm. As the temperature is lowered to –190°C a new emission appears with a maximum near 420 nm.

Although solvent relaxation usually proceeds faster at higher temperatures, high temperature can also prevent the alignment of solvent dipoles. This effect can also prevent

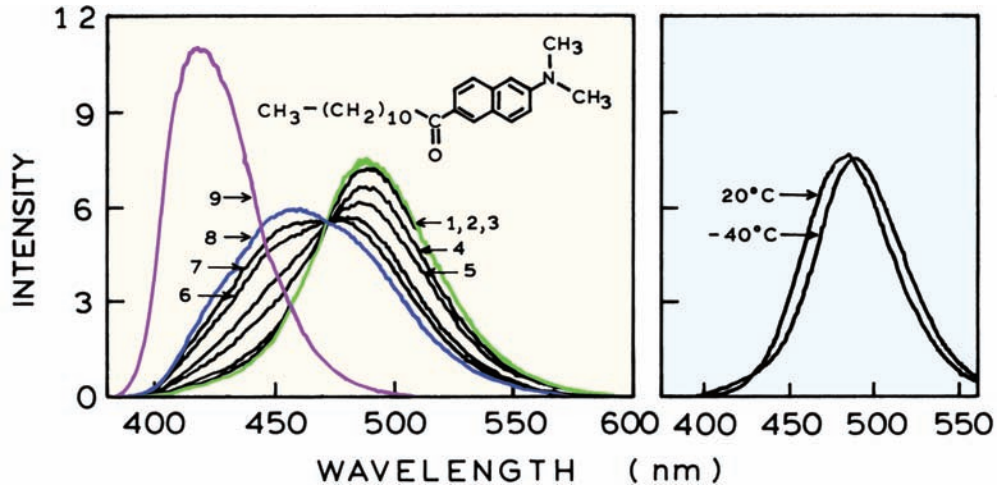

Figure 6.28. Emission spectra of Laurdan in ethanol at –50°C (1), –60°C (2), –70°C (3), –80°C (4), –85°C (5), –90°C (6), –100°C (7), –110°C (8), and –190°C (9). The panel on the right compares the emission spectra of Laurdan at –40 and 20°C. Revised from [56].

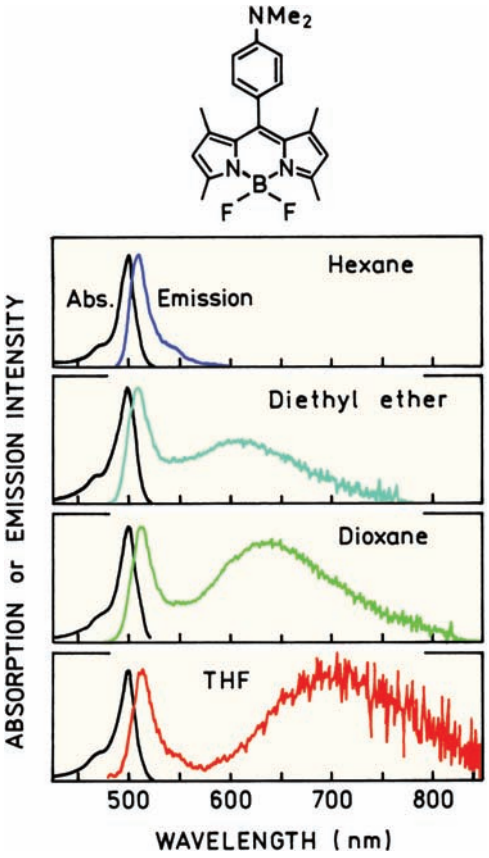

Figure 6.29. Emission spectra of a dimethylamino-substituted Bodipy probe. Tetrahydrofuron (THF). Revised and reprinted with permission from [67]. Copyright © 1998, American Chemical Society.

the alignment of solvent dipoles. This effect is seen for Laurdan in ethanol at 20°C (Figure 6.28, right). This emission spectrum is blue-shifted relative to the emission spectrum in ethanol at –40°C. In general, the most pronounced red shifts occur at temperatures at which the solvent is fluid enough to reorient prior to fluorescence emission but thermal energy is not so great as to disrupt these orientations.

The unusual temperature-dependent spectra displayed by Laurdan were explained by the presence of emission from the locally excited (LE) state and from the internal charge-transfer (ICT) state. In the LE state the excitation is localized on the naphthalene ring, so that the molecule is not very polar. In this LE state the amino and carbonyl groups are not part of the delocalized electron system. At higher temperature the ICT state forms, with complete charge transfer from the amino group to the carbonyl group. Some authors propose that twisting of the dimethyl amino group is required to allow the nitrogen electrons to be in conjugation with the naphthalene ring.[57–58] Hence, the large spectral shift displayed by Prodan-like molecules is somewhat misleading. Part of the shift from 420 to 455 nm is due to formation of the TICT state. The remaining shift from 455 to 490 nm is due to the orientation polarizability (Δf) of the solvent. Prodan is just one example of a large number of molecules that display ICT emission.[59–66]

Formation of ICT states can also occur with some of the more recently developed fluorophores. Figure 6.29 shows the emission spectra of a Bodipy fluorophore that has been substituted with a dimethylamino group.[67] In a low-polarity solvent the usual narrow Bodipy emission is seen with a small Stokes shift. In slightly more polar solvents a new longer wavelength emission is seen that is due to an ICT state. The important point from these examples is that the spectral shifts due to formation of ICT states are not explained by the Lippert equation. Instead of polarity, the appearance of the ICT emission depends on the electron-donating and -accepting properties of groups within or attached to the fluorophore.

6.6.2. Excited-State Intramolecular Proton Transfer (ESIPT)

The formation of ICT states indicates that the electron distribution can be different for a fluorophore in the ground or excited states. This can result in changes of ionization in the excited state. One example is intramolecular proton transfer in the excited state, which is referred to as ESIPT. This is shown in the top schematic in Figure 6.30, for the probe FA.[70] This probe can exist in the normal form (N) or as a tautomer (T). The process of ESIPT can be very rapid because the transferring proton is already next to the proton acceptor at the moment of excitation.

Figure 6.30 shows the emission spectra of FA when dissolved in two nonpolar solvents and when in aqueous solution but bound to BSA. The emission near 525 nm is the N* form, and the emission near 625 nm is the T* form. FA exhibits very low fluorescence in water, but it is highly fluorescent when bound to BSA. This high intensity and the similar intensities of the N* and T* forms indicate that FA is in a highly nonpolar environment when bound to BSA. The relative intensities of the N* and T* emission can be expected to be dependent on the detailed charge and polarity surrounding the fluorophore, as well as its extent of exposure to the aqueous phase. ESIPT occurs in a variety of other fluorophores.[68-77]

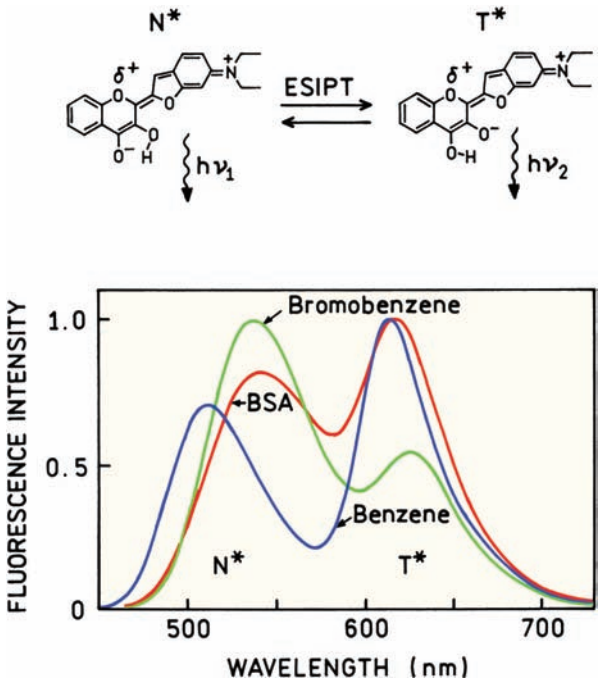

Figure 6.30. Emission spectra of FA that undergoes ESIPT. Revised from [70].

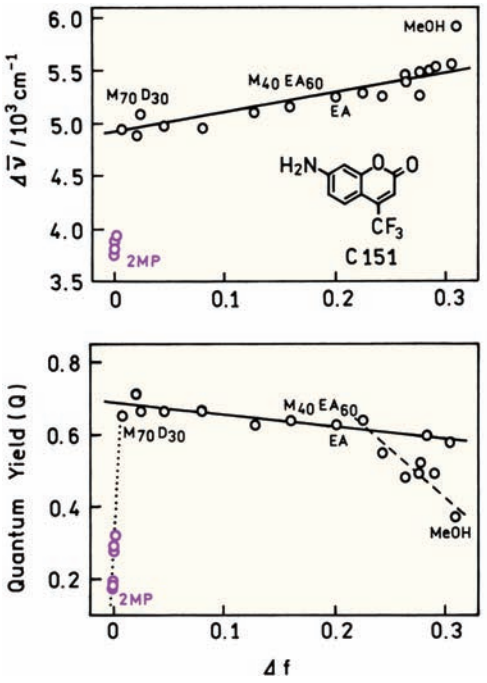

Figure 6.31. Stokes shifts and quantum yields for Coumarin-151 in various solvents. 2-MP, 2-methylpentane; $M_{70}D_{30}$, 70% 2-MP and 30% dioxane (D); $M_{60}EA_{40}$, 60%, 2 MP and 40% EA, ethyl acetate; MeOH, methanol. The composition of the solvents is only listed for several of the mixtures. Revised and reprinted with permission from [78]. Copyright © 2001, American Chemical Society.

6.6.3. Changes in the Non-Radiative Decay Rates

In the previous example the probe FA displayed a very low quantum yield in water but a high quantum yield when bound to BSA. Increases in quantum yield are frequently observed when fluorophores bind to biomolecules. These changes are due to solvent or environmental effects, but these changes are not explained by the Lippert equation. It seems reasonable to suggest that changes in quantum yield are due to changes in the rates of non-radiative decay (k_{nr}). This suggestion is correct, and changes in k_{nr} have been observed for a variety of fluorophores. One example is coumarin-151 (C151), which is highly sensitive to solvent polarity.[78] Figure 6.31 shows the Stokes shift and quantum yields for C151 in solvents ranging from 2-methylpentane ($\Delta f = 0$) to methanol ($\Delta f = 0.309$). The Stokes shift increases in a stepwise manner upon addition of the polar solvent dioxane, even though the value of Δf is almost unchanged. The quantum yield is low in nonpolar solvents and also increases stepwise when the solvent contains a polar additive. Since the excitation coefficient and radiative decay rates are usually not very sensitive to solvent polarity, the decrease in quantum yield suggests an increase in k_{nr} in nonpolar solvents. The values of the radiative (Γ) and non-radiative (k_{nr}) decay rates can be calculated using the measured quantum yields (Q) and lifetimes (τ). These rate constants are given by

$$k_{nr} = (1 - Q)/\Gamma \tag{6.21}$$

$$G = Q/\Gamma \tag{6.22}$$

Figure 6.32 shows the lifetimes of C151 and the calculated rate constants. As expected Γ (○) is mostly independent of solvent polarity. The value of k_{nr} (●) increases dramatically in low-polarity solvents. The authors attribute the increased value of k_{nr} in nonpolar solvents to rotation of the amino group, which provides a rapid deactivation pathway to the ground state. In more polar solvents an ICT state is formed, which causes the larger Stokes shift. In this ICT state, rotation of the amino group is restricted and k_{nr} is smaller. The purpose of this example is not to explain the detailed photophysics of C151, but rather to show how the chemical structures of the fluorophore and the solvent can

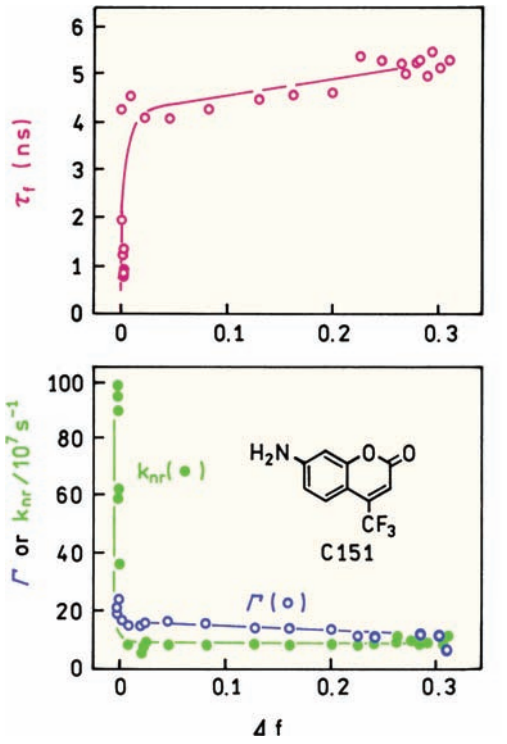

Figure 6.32. Lifetimes, radiative, and non-radiative decay rates for C151 in various solvents. Revised and reprinted with permission from [78]. Copyright © 2001, American Chemical Society.

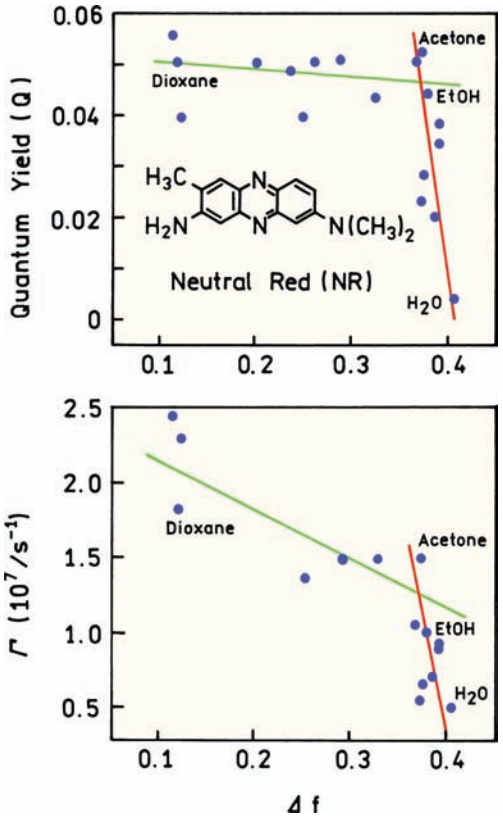

Figure 6.33. Quantum yields and radiative decay rates of Neutral Red in various solvents. Revised from [79].

result in specific interactions that affect the emission maxima and quantum yields of fluorophores.

6.6.4. Changes in the Rate of Radiative Decay

In the previous example the quantum yield of C151 decreases in low polarity solvents. A more typical situation is an increase in quantum yield in low-polarity solvents, which is illustrated by the probe neutral red (NR).[79] For this probe the Lippert plot is biphasic and shows a larger slope for high-polarity solvents ($\Delta f > 0.35$ in Figure 6.33). This behavior is explained by formation of an ICT state in high-polarity solvents, and emission from an LE state in lower-polarity solvents. The slopes of the Lippert plots for NR are consistent with excited-state dipole moments of 4.8D for the LE state and 17.5D for the ICT state. There appears to be a decrease in the radiative decay rate in the higher-polarity solvents. Such a decrease in Γ is possible because the ICT emission is from a different electronic state than the LE emission.

The spectral properties of NR can be understood by considering the energy of the LE and ICT states in solvents of different polarity (Figure 6.34). In low-polarity solvents the LE state has a lower energy. In higher-polarity solvents the ICT state is stabilized by interaction with the solvent and thus becomes the emitting species. These examples of C151 and NR show that no single model or interaction can explain the diverse spectral properties displayed by fluorophores in various environments.

6.7. EFFECTS OF VISCOSITY

Viscosity can have a dramatic effect on the emission intensity of fluorophores. Perhaps the best-known example is trans-stilbene. The intensity decays of stilbene (Figure 6.35) are strongly dependent on temperature.[80] This effect has been interpreted as due to rotation about the central ethylene double bond in the excited state (Figure 6.36).[81–82] In the ground state there is a large energy barrier to rotation about this bond. The energy barrier is much smaller in the excited state. Rotation about this bond occurs in about 70 ps, providing a return path to the ground state. Rotation of

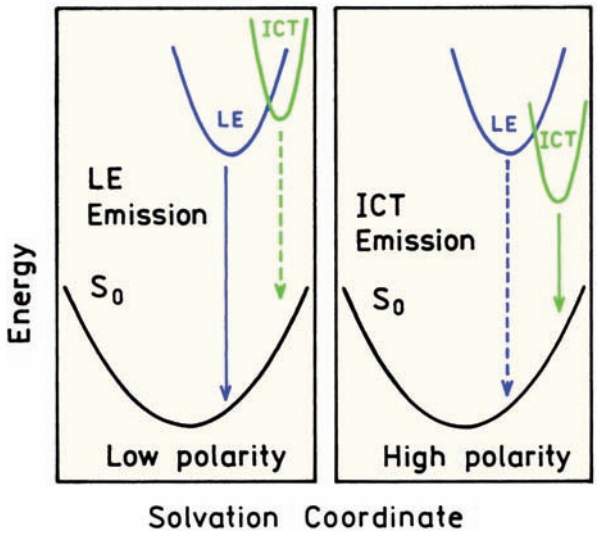

Figure 6.34. Effect of solvent polarity on the energies of LE and ICT states. Revised from [79].

cis-stilbene is even more rapid, resulting in very short fluorescence lifetime. Such rotations in the excited state are thought to affect the emission of many other fluorophores.[83]

Increase in local viscosity contributes to the increased intensities displayed by many fluorophores when bound to biomolecules. In Chapter 1 we mentioned the viscosity probe CCVJ, which displayed increases in quantum yield with increases in viscosity. Figure 6.37 shows the emission intensities of this probe when bound to an antibody directed against this probe.[84] Binding of CCVJ to the antibody prevents rotation around the ethylene bond and increases the quantum yield.

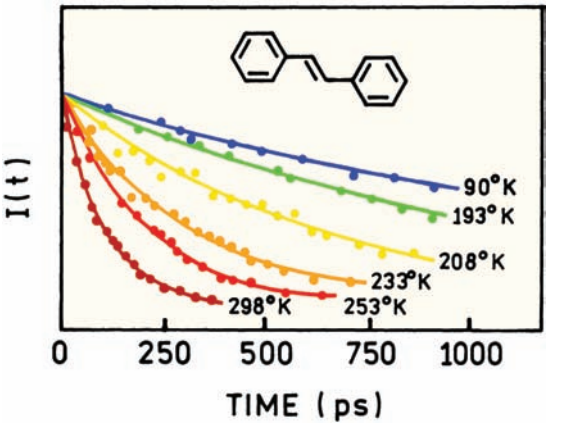

Figure 6.35. Intensity decays of trans-stilbene in methylcyclohexane: isohexane (3:2). Revised from [80].

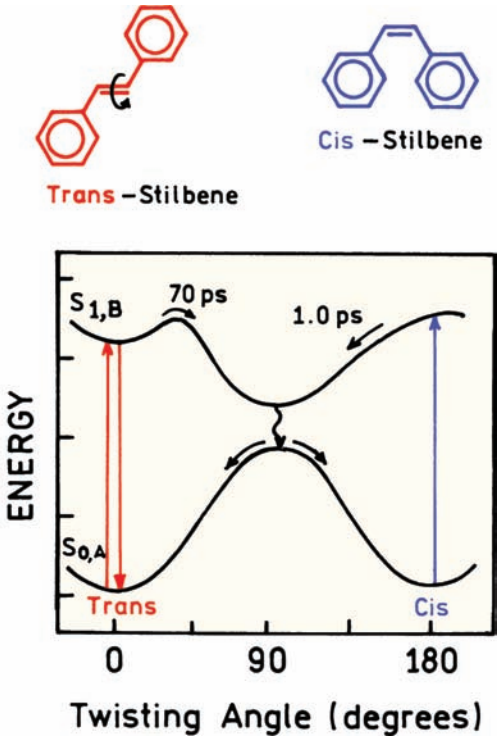

Figure 6.36. Excited-state isomerization of stilbene. From [81].

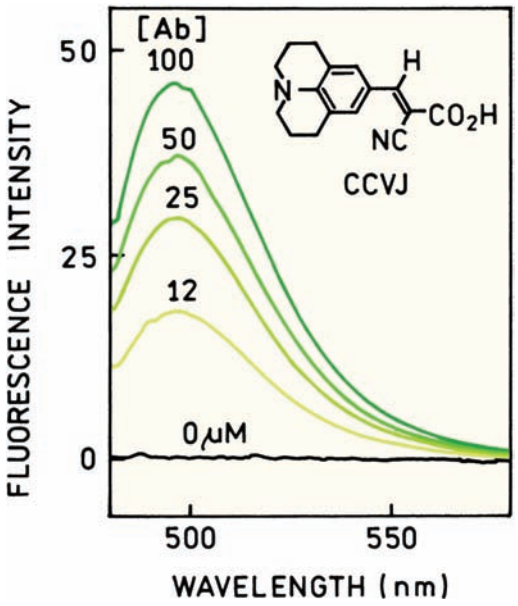

Figure 6.37. Effect of anti-CCVJ antibody on the emission of CCVJ. Antibody concentrations are shown in μM. Revised and reprinted with permission from [84]. Copyright © 1993, American Chemical Society.

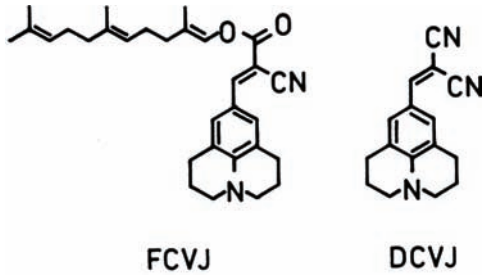

Figure 6.38. Chemical structures of viscosity-sensitive fluorophores. The carbon chain on the left is a farnesol group. Revised from [86].

6.7.1. Effect of Shear Stress on Membrane Viscosity

The viscosity of some membranes are thought to be sensitive to the shear stresses created by fluid flow.[85] This possibility was tested using the viscosity probes shown in Figure 6.38. DCVJ was expected to be more water soluble and FCVJ was expected to label cell membranes. The locations of these probes in human epidermal cells were determined by recording images at various heights in the cells (z-axis sectioning). Figure 6.39 shows pseudocolor images of the labeled cells. Blue indicates images recorded in a plane passing through the center of the cells and thus staining of the cytoplasm. Red indicates images recorded in a plane across the top of the cells, and thus staining of the plasma membrane. These images show that FCVJ localizes primarily in the plasma membrane (left) and that DCVJ localizes primarily in the cytoplasm.

The fluorescence intensities of DCVJ and FCVJ were examined as the epidermal cells were subjected to shear stress. For DCVJ, which was localized in the cytoplasm, there was no change in intensity (Figure 6.39, lower panel). For FCVJ, which bound to the plasma membrane, there was a large drop in intensity in response to shear stress. The reversibility of the changes with elimination of fluid flow showed that the probes were not being washed out of the cells, indicating a decrease in viscosity. These viscosity-dependent probes thus provide an optical means to follow changes in the microviscosity of cell membranes in response to stimuli.

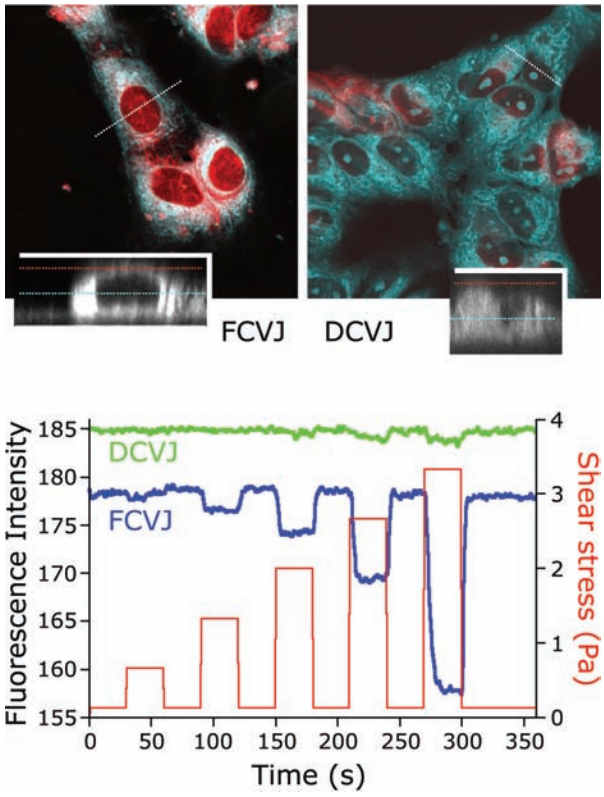

Figure 6.39. Pseudocolor images of human epidermal cells stained with FCVJ or DCVJ. In the images red indicates labeling of the cell membrane and blue indicates labeling of the cytoplasm. The red and blue lines on the inserts indicates the z-level of the images. The lower panel shows the effect of shear stress on the intensities of cells labeled with FCVJ or DCVJ. Revised from [86]. Courtesy of Dr. Emmanuel Theodorakis from the University of California, San Diego.

6.8. PROBE–PROBE INTERACTIONS

In addition to interacting with solvents, fluorophores can interact with each other. One example is excimer formation due to an excited-state complex of two identical fluorophores. Excimer formation is a short-range interaction that requires molecular contact between the fluorophore. In Chapter 1 we described excimer formation by pyrene as a means to measure diffusion in membranes.

Excimer formation is beginning to find use in biotechnology. Figure 6.40 shows the use of excimer formation to detect an insertion mutation in DNA.[87–88] A DNA oligomer was synthesized that contained two nearby pyrene residues. The sequence of this probe was mostly complementary to the target sequence, except for the region near the pyrene groups. When bound to the wild-type (WT) sequence, one of the pyrenes intercalated into the double helix and the second remained outside the double helix. Since the pyrenes were not in contact there was no excimer emission. This probe DNA was then hybridized with a insertion mutant (IM) sequence that contained an extra base. This base prevented the pyrene from intercalating into the double helix, resulting in a blue emission from the excimer.

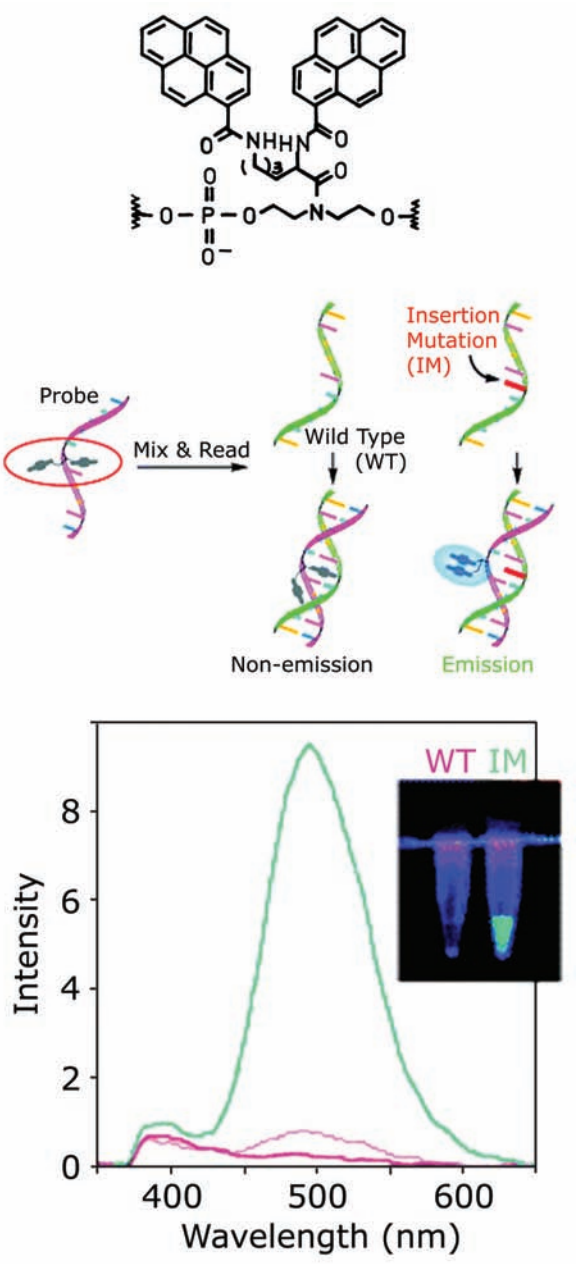

Figure 6.40. Use of excimer formation for detection of a DNA insertion mutation. Top: structure of the probe oligonucleotide. Middle: schematic of the hybridization reaction. Bottom: emission spectra of the probe bound to the wild-type (WT) sequence or the insertion mutation (FM) sequence. Revised and reprinted with permission from [87]. Copyright © 2004, American Chemical Society.

Excimer formation is also finding use in nanotechnology, in particular for following self-assembly processes. Derivatives of perylene were found to self-associate.[89] The extent of self-association depends on the solvent and the starting concentrations of the fluorophore (Figure 6.41, top). Different starting concentrations could be used to obtain a wide range of emission colors (bottom). One can imagine such complexes being used for organic multicolor displays using just a single type of fluorophore.

6.9. BIOCHEMICAL APPLICATIONS OF ENVIRONMENT-SENSITIVE FLUOROPHORES

The use of probes sensitive to this local environment has a long history in biochemical research. We now describe a few examples to illustrate the diversity of these applications.

6.9.1. Fatty-Acid-Binding Proteins

Fatty acids are a significant source of energy. In blood the fatty acids are usually transported bound to serum albumin. In cells the fatty acids are transported by fatty-acid-binding proteins (FABPs), which are a family of small proteins (≈15 kDa) with a variety of amino-acid sequences. Since fatty acids are spectroscopically silent, their association with FABPs is not easily measured.

The problem of detecting fatty acid binding was solved using FABP labeled with acrylodan.[90–94] The structure of acrylodan is shown in Figure 6.22. In the absence of added fatty acid the emission spectrum of acrylodan is blue shifted, indicating a nonpolar environment. Titration of the labeled FABP with fatty acid resulted in a progressive red shift of the emission spectrum (Figure 6.42). Apparently, bound fatty acid displaces this probe from its hydrophobic binding site into the aqueous phase. Displacement of the acrylodan residue from the hydrophobic pocket was supported by a decrease in anisotropy from 0.32 to 0.15 in the presence of bound fatty acid. The spectral shifts were also used to provide a method to measure the concentration of free fatty acids in clinical samples.[95–96]

6.9.2. Exposure of a Hydrophobic Surface on Calmodulin

Calmodulin is involved in calcium signaling and the activation of intracellular enzymes. In the presence of calcium calmodulin exposes a hydrophobic surface, which can interact with other proteins. This surface can also bind hydrophobic probes. Calmodulin was mixed with one of three different probes: 9-anthroxycholine (9-AC), 8-anilino-1-naphthalenesulfonate (ANS), or N-phenyl-1-naphthylamine (NPN).[97] In aqueous solution, these probes are all

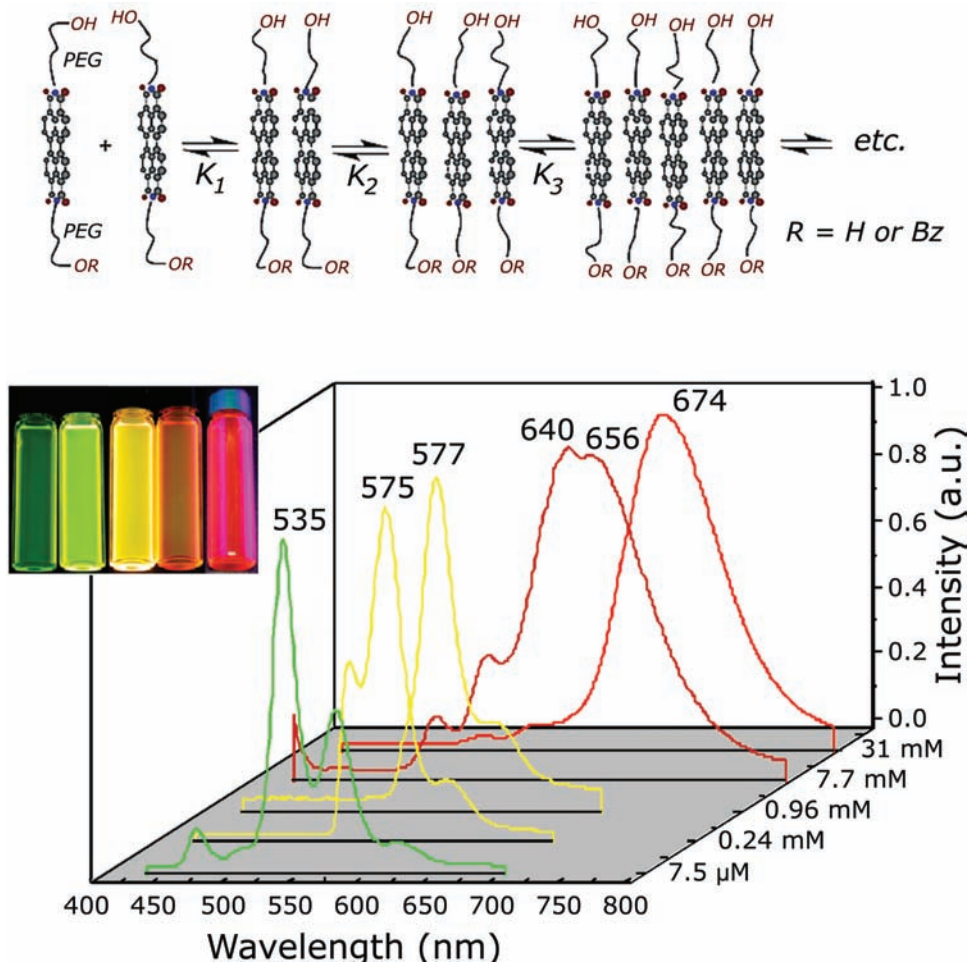

Figure 6.41. Excimer formation by a self-assembled perylene diimide derivative. Revised and reprinted with permission from [89]. Copyright © 2003, American Chemical Society. Courtesy of Dr. Alex D. Q. Li from the Washington State University.

weakly fluorescent in the absence of protein (Figure 6.43). Addition of calmodulin, without calcium, had only a minor effect on the emission. Addition of calcium to calmodulin resulted in a dramatic increase in the intensity of the three probes. Since the effect was seen with neutral (NPN), negatively charged (ANS), and partially charged (9-AC) probes, the binding was interpreted as due to hydrophobic rather than electrostatic interactions between the probe and calmodulin.

6.9.3. Binding to Cyclodextrin Using a Dansyl Probe

While there are numerous examples of proteins labeled with fluorescent probes, relatively few studies are available using labeled carbohydrates.[98–99] The solvent sensitivity of

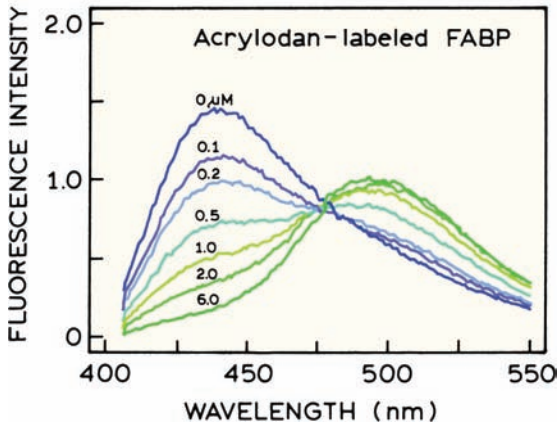

Figure 6.42. Emission spectra of acrylodan-labeled fatty acid binding protein (FABP). The numbers refer to the concentration in µM of fatty acid (oleate) added to 0.2-µM FABP. Revised from [90].

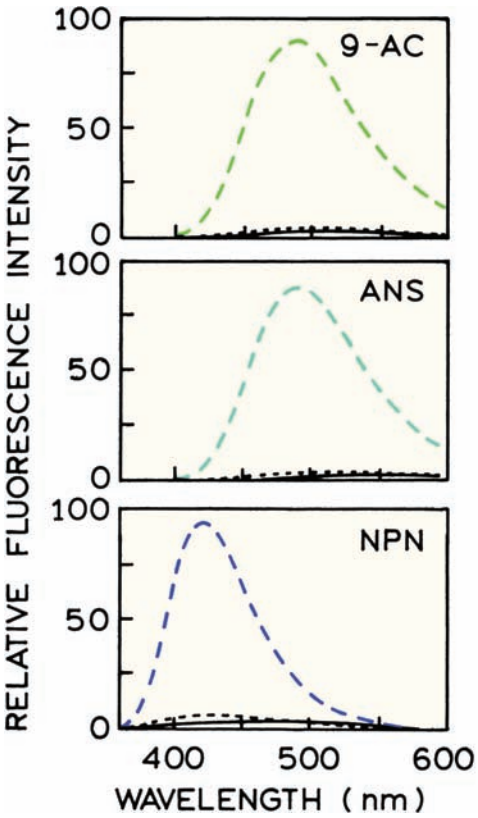

Figure 6.43. Emission spectra of 9-AC, ANS and NPN in aqueous buffer (——), in the presence of calmodulin (- - -), and in the presence of calmodulin plus calcium (– – –). Revised and reprinted with permission from [97]. Copyright © 1980, American Chemical Society.

the dansyl probes have been used to study the binding of organic molecules to cyclodextrins.[98] Cyclodextrins are cyclic sugars. The interior surface of cyclodextrin is hydrophobic, and can bind appropriately sized molecules.

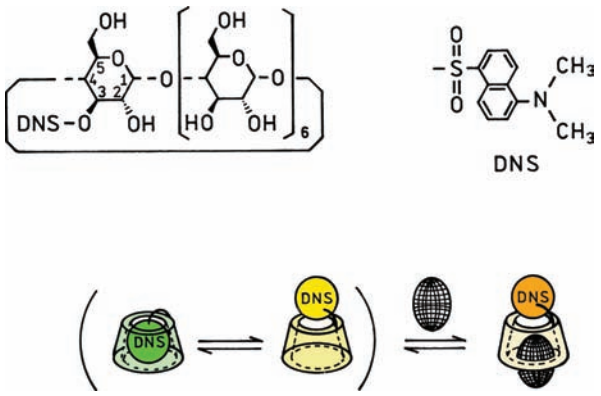

Figure 6.44. Dansyl-labeled cyclodextrin. Also shown is a schematic of the effects of 1-adamantanol (black balls) on the location of the DNS group. Revised from [98].

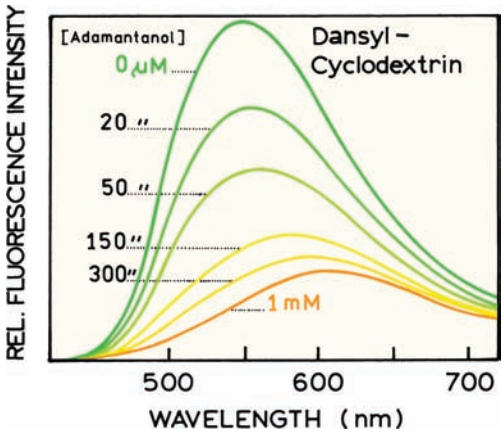

Figure 6.45. Emission spectra of dansyl-cyclodextrin with increasing concentrations of 1-adamantanol. Probe concentrations = 10 M. Revised from [98].

Carbohydrates are not fluorescent. In order to obtain a signal cyclodextrin was labeled with the dansyl group (Figure 6.44). The labeled cyclodextrin was titrated with 1-adamantanol, which resulted in a decrease in fluorescence intensity and a red shift in the emission spectra (Figure 6.45). In the absence of 1-adamantanol the dansyl group binds in the cyclodextrin cavity, resulting in a blue-shifted and enhanced emission. Addition of 1-adamantanol displaces the dansyl group, resulting in greater exposure to the aqueous phase and a red shift in the emission spectra.

6.10. ADVANCED SOLVENT SENSITIVE PROBES

The increased understanding of solvent effects and formation of ICT states has resulted in the development of additional fluorophores that are highly sensitive to solvent polarity.[100–102] These probes are based on 2,5-diphenyloxazole (DPO), which is a well-known scintillator. DPO is soluble mostly in organic solvents, where it displays a high quantum yield. By itself, DPO would not be very sensitive to solvent polarity. Solvent sensitivity was engineered into DPO by the addition of electron donor and acceptor groups (Figure 6.46). The top compound is DPO. In the lower structures the DPO is modified to contain an electron donor, acceptor, or both groups.

Absorption and emission spectra of these four DPO derivatives are shown in Figures 6.47 and 6.48. In methanol, DPO displays structured absorption and emission spectra, with only a small Stokes shift. Addition of the sulfonic acid group alone results in a modest red shift. A larger red shift is observed upon addition of the dimethylamino

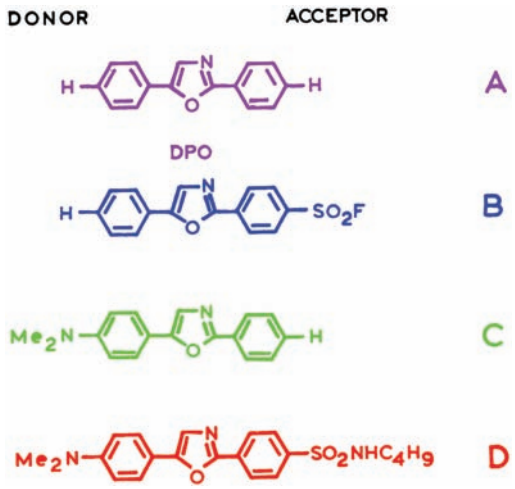

Figure 6.46. Derivatives of 2,5-diphenyloxazole (DPO, A) with donor and acceptor groups (B–D). Revised from [101].

group. The most dramatic shift was found when both electron-donating and -accepting groups were present on the DPO. By addition of both groups the absorption maxima is shifted to more convenient wavelengths near 380 nm, and the emission is shifted to 600 nm. The absence of vibronic structure suggests that the long-wavelength emission is due to an ICT state.

Based on these model compounds, reactive forms of dyes have been prepared, and are called Dapoxyl probes.[102] These probes are highly sensitive to solvent polarity (Figure 6.49). A structured emission is seen in hexane, which disappears in more polar solvents, suggesting that these dyes form ICT states. These dyes are more sensitive to solvent

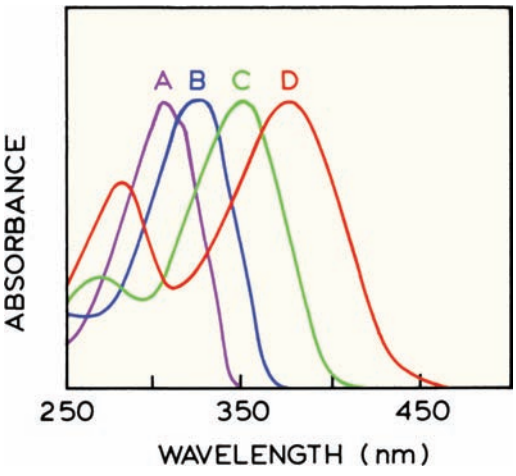

Figure 6.47. Absorption spectra of the DPO derivatives shown in Figure 6.46. The absorption spectra are normalized. From [101].

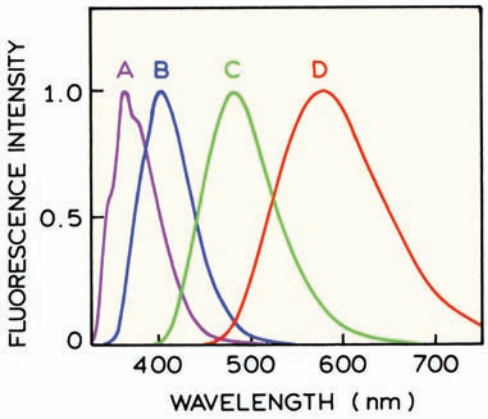

Figure 6.48. Emission spectra of the DPO derivatives shown in Figure 6.46 in methanol. The spectra were normalized. From [101].

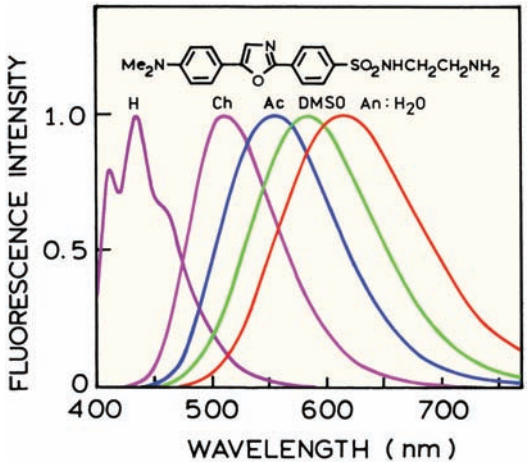

Figure 6.49. Emission spectra of the Dapoxyl SEDA (dapoxyl sulfonyl ethylenediamine) in solvents of increasing polarity, from left to right, hexane (H), chloroform (Ch), acetone (Ac), 1 dimethylsulfoxide (DMSO), and acetonitrile–water (Ac:H_2O, 1:1, vol/vol). From [101].

than other presently used fluorophores (Table 6.3), and they also display usefully high extinction coefficients. In future years one can expect to see increased use of such dyes designed to display large Stokes shifts.

6.11. EFFECTS OF SOLVENT MIXTURES

Advanced Topic

In Section 6.3 we described the phenomena of specific solvent effects, in which small amounts of a polar solvent result in dramatic shifts of the emission spectra. The presence of such effects suggests the presence of a distribution of fluorophores, each with a somewhat different solvent

Table 6.3. Spectral Properties of Well-Known Solvent Sensitive Probes

Probe[a]	λ_{abs} (nm) (ε, M^{-1} cm^{-1})	λ_F (nm) in MeOH	λ_F (nm) in $CHCl_3$	$\Delta\lambda_F$ (nm)
Dapoxyl SEDA	373 (28 000)	584	509	75[b]
Dansyl EDA	335 (4600)	526	499	27
ADMAN	360 (15 000)	499	440	59
Prodan	361 (16 000)	498	440	58
1,8-ANS	372 (7800)	480	490	–10
2,6-ANS	319 (27 000)	422	410	12
7-Ethoxycoumarin	324 (11 000)	399	385	14[b]

[a]Dapoxyl SEDA, dapoxyl sulfonyl ethylenediamine; Dansyl EDA, dansyl ethylenediamine; ADMAN, 6-acetyl-2-dimethylaminonaphthalene; Prodan, 6-propionyl-2-dimethylaminonaphthalene; 1,8-ANS, 8-anilinonaphthalene-1-sulfonic acid; 2,6-ANS, 6-anilinonaphthalene-2-sulfonic acid. From [101].

[b]This value was calculated from λ_F (in MeOH) – λ_F (in $CHCl_3$), which may have been listed incorrectly in [101].

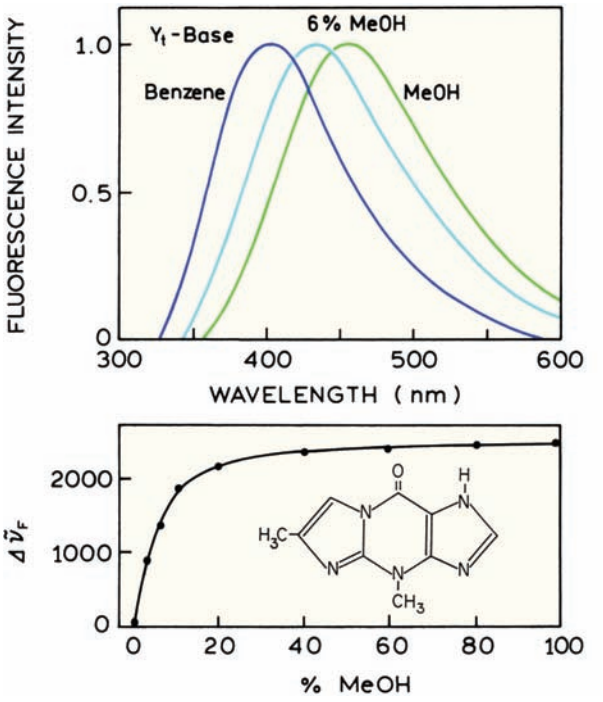

Figure 6.50. Emission spectra of Yt-base in benzene, benzene with 6% methanol, and in methanol. Lower panel, dependence of the spectral shift on the percentage of methanol in benzene. From [105].

shell. Such a distribution of environments can result in complex intensity decays.

The effect of a solvent mixture on an intensity decay is illustrated by Yt-base, which is highly sensitive to solvent polarity.[103–105] The emission maximum of Yt-base shifts from 405 nm in benzene to 455 nm in methanol (Figure 6.50). Addition of only 6% methanol, which does not dramatically change the orientation polarizability Δf, results in a large shift of the emission maximum to 430 nm. A large spectral shift for a small change in the composition of the solvent usually indicates specific solvent effects.

Solvent mixtures provide a natural situation where one can expect a complex intensity decay, or a distribution of lifetimes. The intensity decay of Yt-base in pure benzene or methanol is mostly a single exponential (Table 6.4). However, the decay times are different in each solvent, so that one can expect a more complex decay in a benzene–methanol mixture. In fact, a more heterogeneous intensity decay was observed in benzene with 6% methanol than in either pure solvent. This can be seen by the elevated value of χ_R^2 for the single-decay-time fit for the intensity decay of Yt-base with 6% methanol (Table 6.4). Use of the double-exponential model reduces χ_R^2 from 8.9 to 1.2.

While the intensity decays of Yt-base could be fit using a two-decay-time model, it seems unlikely that there would be only two decay times in a solvent mixture. Since the solvent mixture provides a distribution of environments for the fluorophores, one expects the intensity decay to display a distribution of lifetimes. The frequency response of Yt-base in the solvent mixture could not be fit to a single decay time (Figure 6.51). However, the data also could be fit to a distribution of lifetimes (Figure 6.52). In 100% benzene or 100% methanol the intensity decays were described by narrow lifetime distributions, which are essentially the same as a single decay time. In benzene–methanol mixtures, wide lifetime distributions were needed to fit the intensity decay (Figure 6.52). Lifetime distributions can be expected for any macromolecule in which there exists a distribution of fluorophore environments.

It is interesting to notice that the χ_R^2 values are the same for the multi-exponential and for the lifetime distribution fits for Yt-base with 6% methanol. This illustrates a frequently encountered situation where different models yield

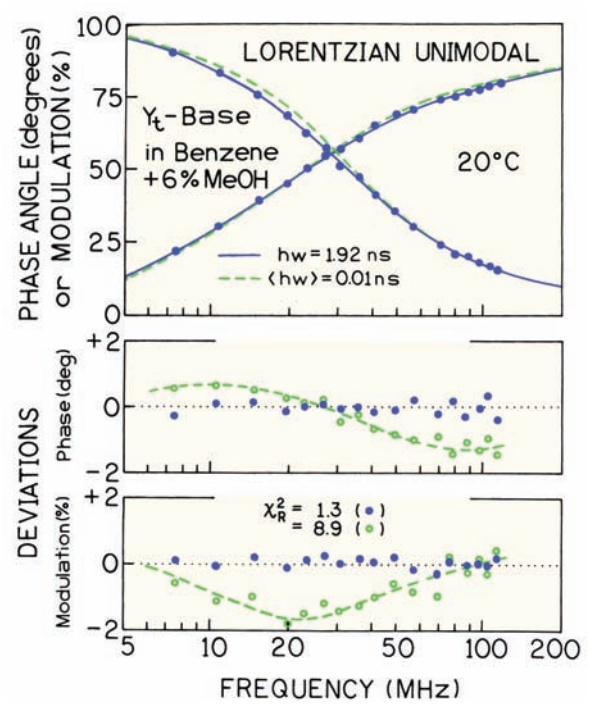

Figure 6.51. Frequency-domain intensity decay of Yt-base in benzene with 6% methanol. From [103].

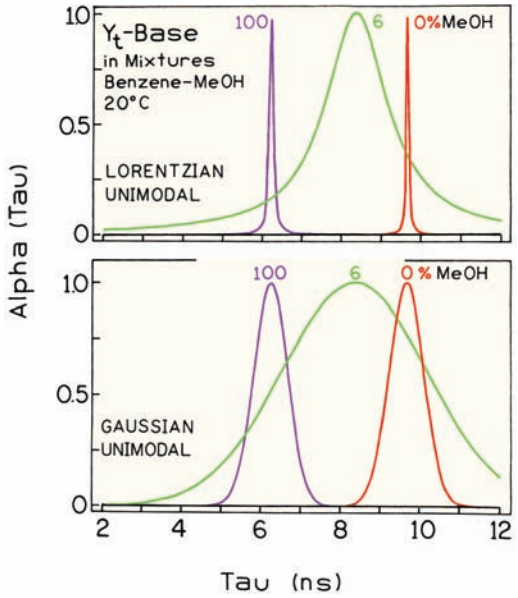

Figure 6.52. Lifetime distribution analysis of the intensity decay of Yt-base in pure methanol, pure benzene, and benzene with 6% methanol. Revised from [103].

equivalent fits. In such cases one must rely on other information to select the more appropriate model. In this case the lifetime distribution model seems preferable because there is no reason to expect two unique decay times in a solvent mixture.

6.12. SUMMARY OF SOLVENT EFFECTS

A quantitative description of the effects of environment on fluorescence emission spectra is perhaps the most challenging topic in fluorescence spectroscopy. No single theory or type of interactions can be used in all circumstances. A number of factors affect the emission including:

Table 6.4. Multi-Exponential Analysis of the Intensity Decays of Yt-Base in Benzene/Methanol Mixtures[a]

% Methanol	Number of decay times	τ_i (ns)	α_i	f_i	x_2^R
0		9.67	1.0	1.0	1.3
4	1	8.80	1.0	1.0	3.2
	2	3.67	0.061	0.026	1.2
		9.10	0.939	0.974	
6	1	8.36	1.0	1.0	8.9
	2	3.50	0.113	0.048	1.2
		8.92	0.887	0.952	
10	1	7.23	1.0	1.0	4.9
	2	2.99	0.082	0.034	1.0
		7.56	0.918	0.966	
100	1	6.25	1.0	1.0	1.9

[a]From [103].

1. General solvent effects due to the interactions of the dipole of the fluorophore with its environment
2. Specific solvent effects due to fluorophore–solvent interactions
3. Formation of ICT or TICT states depending on the probe structure and the surrounding solvent
4. Viscosity and changes in the radiative and nonradiative decay rates
5. Probe-probe interactions

Even if only one type of interaction were present, the effects would still be complex and beyond the limits of most models. For instance, the Lippert equation is only an approximation, and ignores higher-order terms. Also, this equation only applies to a spherical dipole in a spherical cavity. More complex expressions are needed for nonspherical molecules, but one cannot generally describe the fluorophore shape in adequate detail. With regard to specific effects, there is no general theory to predict the shift in emission spectra due to hydrogen bond formation. And, finally, for fluorophores bound to macromolecules or in viscous solvents, spectral relaxation can occur during emission, so that the emission spectrum represents some weighted average of the unrelaxed and relaxed emission.

Given all these complexities, how can one hope to use the data from solvent sensitive probes? In our opinion, the best approach is to consider the fluorophore structure rather than to rely completely on theory. Observed effects should be considered within the framework of the interactions listed above. Unusual behavior may be due to the presence of more than one type of interaction. Use the theory as an aid to interpreting plausible molecular interactions, and not as a substitute for careful consideration probe structure and its likely chemical interactions.

REFERENCES

1. Safarzadeh-Amiri A, Thompson M, Krull UJ. 1989. Trans-4-dimethylamino-4'-(1-oxobutyl)stilbene: a new fluorescent probe of the bilayer lipid membrane. *J Photochem Photobiol A: Chem* **47**:299–308.
2. Lippert Von E. 1957. Spektroskopische bistimmung des dipolmomentes aromatischer verbindungen im ersten angeregten singulettzustand. *Z Electrochem* **61**:962–975.
3. Mataga N, Kaifu Y, Koizumi M. 1956. Solvent effects upon fluorescence spectra and the dipole moments of excited molecules. *Bull Chem Soc Jpn* **29**:465–470.
4. Rettig W. 1986. Charge separation in excited states of decoupled systems: TICT compounds and implications regarding the development of new laser dyes and the primary processes of vision and photosynthesis. *Angew Chem, Int Ed* **25**:971–988.
5. Bayliss NS. 1950. The effect of the electrostatic polarization of the solvent on electronic absorption spectra in solution. *J Chem Phy* **18**(3):292–296.
6. Bayliss NS, McRae EG. 1954. Solvent effects in organic spectra: dipole forces and the Franck-Condon principle. *J Phys Chem* **58**:1002–1006.
7. McRae EG. 1956. Theory of solvent effects of molecular electronic spectra: frequency shifts. *J Phys Chem* **61**:562–572.
8. Griffiths DJ. 1999. *Introduction to electrodynamics*. Prentice-Hall, Englewood Cliffs, NJ.
9. Kawski A. 1992. Solvent-shift effect of electronic spectra and excited state dipole moments. In *Progress in photochemistry and photophysics*, pp. 1–47. Ed JF Rabek, CRC Press, New York.
10. Seliskar CJ, Brand L. 1971. Electronic spectra of 2-aminonaphthalene-6-sulfonate and related molecules, II: effects of solvent medium on the absorption and fluorescence spectra. *J Am Chem Soc* **93**:5414–5420.
11. Suppan P. 1990. Solvatochromic shifts: the influence of the medium on the energy of electronic states. *J Photochem Photobiol A: Chem* **50**:293–330.
12. Bakhshiev NG. 1961. Universal molecular interactions and their effect on the position of the electronic spectra of molecules in two component solutions, I: theory (liquid solutions). *Opt Spectrosc* **10**:379–384.
13. Bakhshiev NG. 1962. Universal molecular interactions and their effects on the position of electronic spectra of molecules in two-component solutions, IV: dependence on the magnitude of the Stokes shift in the solvent luminescence spectrum (liquid solutions). *Opt Spectrosc* **12**:309–313.
14. Bakhshiev NG. 1962. Universal intermolecular interactions and their effect on the position of the electronic spectra of molecules in two-component solutions. *Opt Spectrosc* **13**:24–29.
15. Kawski A. 2002. On the estimation of excited-state dipole moments from solvatochromic shifts of absorption and fluorescence spectra. *Z Naturforsch A* **57**:255–262.
16. Weber G, Laurence DJR. 1954. Fluorescent indicators of absorption in aqueous solution and on the solid phase. *Biochem J* **56**:XXXI.
17. Slavik J. 1982. Anilinonaphthalene sulfonate as a probe of membrane composition and function. *Biochim Biophys Acta* **694**:1–25.
18. McClure WO, Edelman GM. 1954. Fluorescent probes for conformational states of proteins, I: mechanism of fluorescence of 2-p-toluidinylnaphthalene-6-sulfonate, a hydrophobic probe. *Biochemistry* **5**:1908–1919.
19. Brand L, Seliskar CJ, Turner DC. 1971. The effects of chemical environment on fluorescence probes. In *Probes of structure and function of macromolecules and membranes*, pp. 17–39. Ed B Chance, CP Lee, J-K Blaisie. Academic Press, New York.
20. Turner DC, Brand L. 1968. Quantitative estimation of protein binding site polarity: fluorescence of N-arylaminonaphthalenesulfonates. *Biochemistry* **7**(10):3381–3390.
21. Perov AN. 1980. Energy of intermediate pair interactions as a characteristic of their nature: theory of the solvato (fluoro) chromism of three-component solutions. *Opt Spectrosc* **49**:371–374.
22. Neporent BS, Bakhshiev NG. 1960. On the role of universal and specific intermolecular interactions in the influence of the solvent on the electronic spectra of molecules. *Opt Spectrosc* **8**:408–413.
23. Petrov NK, Markov DE, Gulakov MN, Alfimov MV, Staerk H. 2002. Study of preferential solvation in binary mixtures by means of frequency-domain fluorescence spectroscopy. *J Fluoresc* **12**(1):19–24.
24. Petrov NK, Wiessner A, Staerk H. 2001. A simple kinetic model of preferential solvation in binary mixtures. *Chem Phys Lett* **349**:517–520.

25. Schulman SG, Townsend RW, Baeyens WRG. 1995. Proton-transfer kinetics of photoexcited 2-hydroxybiphenyl in aqueous methanol solutions. *Anal Chim Acta* **303**:25–29.
26. Kim S, Chang DW, Park SY, Kawai H, Nagamura T. 2002. Excited-state intramolecular proton transfer in a dendritic macromolecular system: poly(aryl ether) dendrimers with phototautomerizable quinoline core. *Macromolecules* **35**:2748–2753.
27. Carmona C, Balón M, Galán M, Guardado P, Munoz MA. 2002. Dynamic Study of excited state hydrogen-bonded complexes of harmane in cyclohexane-toluene mixtures. *Photochem Photobiol* **76**(3):239–246.
28. Molotsky T, Huppert D. 2002. Solvation statics and dynamics of coumarin 153 in hexane-propionitrile solvent mixtures. *J Phys Chem A* **106**:8525–8530.
29. Fery-Forgues S, Fayet J-P, Lopez A. 1993. Drastic changes in the fluorescence properties of NBD probes with the polarity of the medium: involvement of a TICT state. *J Photochem Photobiol A: Chem* **70**: 229–243.
30. Mazères S, Schram V, Tocanne J-F, Lopez A. 1996. 7-nitrobenz-2-oxa-1,3-diazole-4-yl-labeled phospholipids in lipid membranes: differences in fluorescence behavior. *Biophys J* **71**:327–335.
31. Cherkasov AS. 1960. Influence of the solvent on the fluorescence spectra of acetylanthracenes. *Akad Nauk SSSR Bull Phys Sci* **24**:597–601.
32. Tamaki T. 1982. The photoassociation of 1- and 2-acetylanthracene with methanol. *Bull Chem Soc Jpn* **55**:1761–1767.
33. Tamaki T. 1980. Polar fluorescent state of 1- and 2-acylanthracenes, II: The perturbation of protic solvents. *Bull Chem Soc Jpn* **53**: 577–582.
34. Perochon E, Tocanne J-F. 1991. Synthesis and phase properties of phosphatidylcholine labeled with 8-(2-anthroyl)-octanoic acid, a solvatochromic fluorescent probe. *Chem Phys Lipids* **58**:7–17.
35. Perochon E, Lopez A, Tocanne JF. 1991. Fluorescence properties of methyl 8-(2-anthroyl) octanoate, a solvatochromic lipophilic probe. *Chem Phys Lipids* **59**:17–28.
36. Rosenberg HM, Eimutus E. 1966. Solvent shifts in electronic spectra, I: Stokes shift in a series of homologous aromatic amines. *Spectrochim Acta* **22**:1751–1757.
37. Werner TC, Hercules DM. 1969. The fluorescence of 9-anthroic acid and its esters: environmental effects on excited-state behavior. *J Phys Chem* **73**:2005–2011.
38. Werner TC, Hoffman RM. 1973. Relation between an excited state geometry change and the solvent dependence of 9-methyl anthroate fluorescence. *J Phys Chem* **77**:1611–1615.
39. Badea MG, De Toma RP, Brand L. 1978. Nanosecond relaxation processes in liposomes. *Biophys J* **24**:197–212.
40. Lakowicz JR, Balter A. 1982. Direct recording of the initially excited and the solvent relaxed fluorescence emission of a tryptophan derivative in viscous solution by phase-sensitive detection of fluorescence. *Photochem Photobiol* **36**:125–132.
41. Lakowicz JR, Bevan DR, Maliwal BP, Cherek H, Balter A. 1983. Synthesis and characterization of a fluorescence probe of the phase transition and dynamic properties of membranes. *Biochemistry* **22**:5714–5722.
42. Weber G, Farris FJ. 1979. Synthesis and spectral properties of a hydrophobic fluorescent probe: 6-propionyl-2-(dimethylamino)-naphthalene. *Biochemistry* **18**:3075–3078.
43. Sire O, Alpert B, Royer CA. 1996. Probing pH and pressure effects of the apomyoglobin heme pocket with the 2'-(N,N-dimethylamino)-6-naphthoyl-4-trans-cyclohexanoic acid fluorophore. *Biophys J* **70**:2903–2914.
44. Prendergast FG, Meyer M, Carlson GL, Iida S, Potter JD. 1983. Synthesis, spectral properties, and use of 6-acryloyl-2-dimethylaminonaphthalene (acrylodan). *J Biol Chem* **258**:7541–7544.
45. Hendrickson HS, Dumdei EJ, Batchelder AG, Carlson GL. 1987. Synthesis of prodan-phosphatidylcholine, a new fluorescent probe, and its interactions with pancreatic and snake venom phospholipases A_2. *Biochemistry* **26**:3697–3703.
46. Sandez MI, Suarez A, Rios MA, Balo MC, Fernandez F, Lopez C. 1996. Spectroscopic study of new fluorescent probes. *Photochem Photobiol* **64**(3):486–491.
47. Lobo BC, Abelt CJ. 2003. Does PRODAN possess a planar or twisted charge-transfer excited state? Photophysical properties of two PRODAN derivatives. *J Phys Chem A* **107**:10938–10943.
48. Hutterer R, Hof M. 2002. Probing ethanol-induced phospholipid phase transitions by the polarity sensitive fluorescence probes prodan and patman. *Z Phys Chem* **216**:333–346.
49. Parasassi T, Gratton E, Yu WM, Wilson P, Levi M. 1997. Two-photon fluorescence microscopy of laurdan generalized polarization domains in model and natural membranes. *Biophys J* **72**:2413–2429.
50. Parasassi T, Krasnowska EK, Bagatolli LA, Gratton E. 1998. Laurdan and prodan as polarity-sensitive fluorescent membrane probes. *J Fluoresc* **8**(4):365–373.
51. Bagatolli LA, Gratton E, Khan TK, Chong PLG. 2000. Two-photon fluorescence microscopy studies of bipolar tetraether giant liposomes from thermoacidophilic archaebacteria *sulfolobus acidocaldarius*. *Biophys J* **79**:416–425.
52. Bondar OP, Rowe ES. 1999. Preferential interactions of fluorescent probe prodan with cholesterol. *Biophys J* **76**:956–962.
53. Bagatolli LA, Gratton E. 2000. Two-photon fluorescence microscopy of coexisting lipid domains in giant unilameller vesicles of binary phospholipid mixtures. *Biophys J* **78**:290–305.
54. Gaus K, Gratton E, Kable EPW, Jones AS, Gelissen I, Kritharides L, Jessup W. 2003. Visualizing lipid structure and raft domains in living cells with two-photon microscopy. *Proc Natl Acad Sci USA* **100**(26):15554–15559.
55. Yoshihara T, Druzhinin SI, Zachariasse KA. 2004. Fast intramolecular charge transfer with a planar rigidized electron donor/acceptor molecule. *J Am Chem Soc* **126**:8535–8539.
56. Viard M, Gallay J, Vincent M, Meyer O, Robert B, Paternostre M. 1997. Laurdan solvatochromism: solvent dielectric relaxation and intramolecular excited-state reaction. *Biophys J* **73**:2221–2234.
57. Nowak W, Sygula A, Adamczak P, Balter A. 1986. On the possibility of fluorescence from twisted intramolecular charge transfer states of 2-dimethylamino-6-acylnaphthalenes: a quantum-chemical study. *J Mol Struct* **139**:13–23.
58. Balter A, Nowak W, Pawelkiewicz W, Kowalczyk A. 1988. Some remarks on the interpretation of the spectral properties of prodan. *Chem Phys Lett* **143**:565–570.
59. Rettig W, Lapouyade R. 1994. Fluorescence probes based on twisted intramolecular charge transfer (TICT) states and other adiabatic photoreactions. In *Topics in fluorescence spectroscopy*, Vol. 4: *Probe design and chemical sensors*, pp. 109–149. Ed JR Lakowicz. Plenum Press, New York.
60. Corneliβen C, Rettig W. 1994. Unusual fluorescence red shifts in TICT-forming boranes. *J Fluoresc* **4**(1):71–74.
61. Vollmer F, Rettig W, Birckner E. 1994. Photochemical mechanisms producing large fluorescence Stokes shifts. *J Fluoresc* **4**(1):65–69.
62. Rotkiewicz K, Grellmann KH, Grabowski ZR. 1973. Reinterpretation of the anomalous fluorescence of P-N,N-dimethylaminobenzonitrile. *Chem Phys Lett* **19**:315–318.

63. Grabowski ZR, Rotkiewicz K, Siemiarczuk A. 1979. Dual fluorescence of donor-acceptor molecules and the twisted intramolecular charge transfer TICT states. *J Lumin* **18**:420–424.
64. Belletête M, Durocher G. 1989. Conformational changes upon excitation of dimethylamino para-substituted 3H-indoles: viscosity and solvent effects. *J Phys Chem* **93**:1793–1799.
65. Jones G, Jackson WR, Choi C-Y, Bergmark WR. 1985. Solvent effects on emission yield and lifetime for coumarin laser dyes: requirements for a rotatory decay mechanism. *J Phys Chem* **89**: 294–300.
66. Ayuk AA, Rettig W, Lippert E. 1981. Temperature and viscosity effects on an excited state equilibrium as revealed from the dual fluorescence of very dilute solutions of 1-dimethylamino-4-cyanonaphthalene. *Ber Bunsenges Phys Chem* **85**:553–555.
67. Kollmannsberger M, Rurack K, Resch-Genger U, Daub J. 1998. Ultrafast charge transfer in amino-substituted boron dipyrromethene dyes and its inhibition by cation complexation: a new design concept for highly sensitive fluorescent probes. *J Phys Chem A* **102**:10211–10220.
68. Klymchenko AS, Duportail G, Mely Y, Demchenko AP. 2003. Ultrasensitive two-color fluorescence probes for dipole potential in phospholipid membranes. *Proc Natl Acad Sci USA* **100**(20):11219–11224.
69. Klymchenko AS, Duportail G, Ozturk T, Pivovarenko VG, Mely Y, Demchenko AP. 2002. Novel two-band ratiometric fluorescence probes with different location and orientation in phospholipid membranes. *Chem Biol* **9**:1199–1208.
70. Ercelen S, Klymchenko AS, Demchenko AP. 2003. Novel two-color fluorescence probe with extreme specificity to bovine serum albumin. *FEBS Lett* **538**:25–28.
71. Fahrni CJ, Henary MM, VanDerveer DG. 2002. Excited-state intramolecular proton transfer in 2-(2'-tosylaminophenyl)benzimidazole. *J Phys Chem A* **106**:7655–7663.
72. Dennison SM, Guharay J, Sengupta PK. 1999. Intramolecular excited-state proton transfer and charge transfer fluorescence of a 3-hydroxyflavone derivative in micellar media. *Spectrochim Acta Part A* **55**:903–909.
73. Do Cabo JL, Faria HB, Portugal SGM, Silva MAA, Brinn IM. 1999. Excited-state acidity of bifunctional compounds, 7: long distance, solvent-assisted excited-state proton transfer in olivacine. *Photochem Photobiol* **69**(6):664–670.
74. Rampey ME, Halkyard CE, Williams AR, Angel AJ, Hurst DR, Townsend JD, Finefrock AE, Beam CF, Studer-Martinez SL. 1999. A new series of proton/charge transfer molecules: synthesis and spectral studies of 2-(5-aryl-1-carbomethoxy-1*H*-pyrazol-3-yl)phenols. *Photochem Photobiol* **70**(2):176–183.
75. Del Valle JC, Dominguez E, Kasha M. 1999. Competition between dipolar relaxation and double proton transfer in the electronic spectroscopy of pyrroloquinolines. *J Phys Chem A* **103**:2467–2475.
76. Chou PT, Chen YC, Yu WS, Chou YH, Wei CY, Cheng YM. 2001. Excited-state intramolecular proton transfer in 10-hydroxybenzo[h]quinoline. *J Phys Chem A* **105**:1731–1740.
77. Nagaoka S, Nakamura A, Nagashima U. 2002. Nodal-plane model in excited-state intramolecular proton transfer of o-hydroxybenzaldehyde; substituent effect. *J Photochem Photobiol A: Chem* **154**(1): 23–32.
78. Nad S, Pal H. 2001. Unusual photophysical properties of coumarin-151. *J Phys Chem A* **105**(7):1097–1106.
79. Singh MK, Pal H, Bhasikuttan AC, Sapre AV. 1998. Dual solvatochromism of neutral red. *Photochem Photobiol* **68**(1):32–38.
80. Sumitani M, Nakashima N, Yoshihara K, Nagakura S. 1977. Temperature dependence of fluorescence lifetimes of *trans*-stilbene. *Chem Phys Lett* **51**(1):183–185.
81. Todd DC, Jean JM, Rosenthal SJ, Ruggiero AJ, Yang D, Fleming GR. 1990. Fluorescence upconversion study of *cis*-stilbene isomerization. *J Chem Phys* **93**(12):8658–8668.
82. Meier H. 2001. Blue fluorescent exciplexes consisting of *trans*-stilbene and antibodies. *Angew Chem, Int Ed* **40**(10):1851–1853.
83. Rettig W, Lapouyade R. 1994. Fluorescence probes based on twisted intramolecular charge transfer (TICT) states and other adiabatic photoreactions. In *Topics in fluorescence spectroscopy*, Vol. 4: *Probe design and chemical sensing*, pp. 109–149. Ed JR Lakowicz. Plenum Press, New York.
84. Iwaki T, Torigoe C, Noji M, Nakanishi M. 1993. Antibodies for fluorescent molecular rotors. *Biochemistry* **32**:7589–7592.
85. Haidekker MA, L'Heureux N, Frangos JA. 2000. Fluid shear stress increases membrane fluidity in endothelial cells: a study with DCVJ fluorescence. *Am J Physiol Heart Circ Physiol* **278**:H1401–H1406.
86. Haidekker MA, Ling T, Anglo M, Stevens HY, Frangos JA, Theodorakis EA. 2001. New fluorescent probes for the measurement of cell membrane viscosity. *Chem Biol* **8**:123–131.
87. Okamoto A, Ichiba T, Saito I. 2004. Pyrene-labeled oligodeoxynucleotide probe for detecting base insertion by excimer fluorescence emission. *J Am Chem Soc* **126**:8364–8365.
88. Yamana K, Iwai T, Ohtani Y, Sato S, Nakamura M, Nakano H. 2002. Bis-pyrene-labeled oligonucleotides: sequence specificity of excimer and monomer fluorescence changes upon hybridization with DNA. *Bioconjugate Chem* **13**:1266–1273.
89. Wang W, Han JJ, Wang LQ, Li LS, Shaw WJ, Li ADQ. 2003. Dynamic π–π stacked molecular assemblies emit from green to red colors. *Nano Lett* **3**(4):455–458.
90. Richieri GV, Ogata RT, Kleinfeld AM. 1992. A fluorescently labeled intestinal fatty acid binding protein. *J Biol Chem* **267**(33):23495–23501.
91. Richieri GV, Anel A, Kleinfeld AM. 1993. Interactions of long-chain fatty acids and albumin: determination of free fatty acid levels using the fluorescent probe ADIFAB. *Biochemistry* **32**:7574–7580.
92. Richieri GV, Ogata RT, Kleinfeld AM. 1996. Kinetics of fatty acid interactions with fatty acid binding proteins from adipocyte, heart, and intestine. *J Biol Chem* **271**(19):11291–11300.
93. Richieri GV, Ogata RT, Kleinfeld AM. 1996. Thermodynamic and kinetic properties of fatty acid interactions with rat liver fatty acid-binding protein. *J Biol Chem* **271**(49):31068–31074.
94. Richieri GV, Ogata RT, Kleinfeld AM. 1994. Equilibrium constants for the binding of fatty acids with fatty acid-binding proteins from adipocyte, intestine, heart and liver measured with the fluorescent probe ADIFAB. *J Biol Chem* **269**(39):23918–23930.
95. Richieri GV, Kleinfeld AM. 1995. Unbound free fatty acid levels in human serum. *J Lipid Res* **36**:229–240.
96. Kleinfeld AM, Prothro D, Brown DL, Davis RC, Richieri GV, DeMaria A. 1996. Increases in serum unbound free fatty acid levels following coronary angioplasty. *Am J Cardiol* **78**:1350–1354.
97. LaPorte DC, Wierman BM, Storm DR. 1980. Calcium-induced exposure of a hydrophobic surface on calmodulin. *Biochemistry* **19**:3814–3819.
98. Wang Y, Ikeda T, Ikeda H, Ueno A, Toda F. 1994. Dansyl-β-cyclodextrins as fluorescent sensors responsive to organic compounds. *Chem Soc Jpn* **67**:1598–1607.
99. Nagata K, Furuike T, Nishimura S-I. 1995. Fluorescence-labeled synthetic glycopolymers: a new type of sugar ligands of lectins. *J Biochem* **118**:278–284.

100. *BioProbes 25: New Products and Applications*. 1997. Molecular Probes Inc. Eugene, OR. May 1997.
101. Diwu Z, Lu Y, Zhang C, Kalubert DH, Haugland RP. 1997. Fluorescent molecular probes, II: the synthesis, spectral properties and use of fluorescent solvatochromic dapoxyl™ dyes. *Photochem Photobiol* **66**:424–431.
102. Dapoxyl is a trademark of Molecular Probes Inc.
103. Gryczynski I, Wiczk W, Lakowicz JR, Johnson ML. 1989. Decay time distribution analysis of Yt-base in benzene-methanol mixtures. *J Photochem Photobiol B: Biol* **4**:159–170.
104. Gryczynski I, Wiczk W, Johnson ML, Lakowicz JR. 1988. Lifetime distributions and anisotropy decays of indole fluorescence in cyclohexane/ethanol mixtures by frequency-domain fluorometry. *Biophys Chem* **32**:173–185.
105. Gryczynski I. Unpublished observations.

PROBLEMS

P6.1. *Calculation of a Stokes Shift*: Calculate the spectral shift of a fluorophore in methanol with $\mu_E - \mu_G = 14$D and a cavity radius of 4 Å. That is, confirm the values in Table 6.2. Show that the answer is calculated in cm^{-1}. Note, esu = $g^{1/2}$ $cm^{3/2}/s$ and erg = g cm^2/s^2.

P6.2. *Calculation of the Excited State Dipole Moment*: Use the data in Table 6.5 to calculate the change in dipole moment ($\Delta\mu$) of Prodan excited state. Calculate the change in dipole moment $\Delta\mu$ for both the locally excited (LE) and the internal charge-transfer (ICT) state. Assume the cavity radius is 4.2 Å.

Table 6.5. Spectral Properties of PRODAN in Various Solvents[a]

No.	Solvent	Absorption maximum (nm)	Emission maximum (nm)	Stokes shift (cm^{-1})	Δf
1	Cyclohexane	342	401	4302	0.001
2	Benzene	355	421	4416	0.002
3	Triethylamine	343	406	4523	0.102
4	Chlorobenzene	354	430	4992	0.143
5	Chloroform	357	440	5284	0.185
6	Acetone	350	452	6448	0.287
7	Dimethylformamide	355	461	6477	0.276
8	Acetonitrile	350	462	6926	0.304
9	Ethylene glycol	375	515	7249	0.274
10	Propylene glycol	370	510	7419	0.270
11	Ethanol	360	496	7616	0.298
12	Methanol	362	505	8206	0.308
13	Water	364	531	8646	0.302

[a]Data from [42].